Published in final edited form as:
Nature. 2020 September 01; 585(7825): 453–458. doi:10.1038/s41586-020-2706-x.

Epigenetic gene silencing by heterochromatin primes fungal resistance

Sito Torres-Garcia, **Imtiyaz Yaseen**, **Manu Shukla**, **Pauline N. C. B. Audergon**[†], **Sharon A. White**, **Alison L. Pidoux**, **Robin C. Allshire**[*]
Wellcome Centre *for* Cell Biology and Institute of Cell Biology, School of Biological Sciences, The University of Edinburgh, Mayfield Road, Edinburgh EH9 3BF, UK

Summary

Genes embedded in H3 lysine 9 methylation (H3K9me)–dependent heterochromatin are transcriptionally silenced[1–3]. In fission yeast, *Schizosaccharomyces pombe*, H3K9me-mediated heterochromatin can be transmitted through cell division provided the counteracting demethylase Epe1 is absent[4,5]. Under certain conditions wild-type cells might utilize heterochromatin heritability to form epimutations, phenotypes mediated by unstable silencing rather than DNA changes[6,7]. Here we show that resistant heterochromatin-dependent epimutants arise in threshold levels of caffeine. Unstable resistant isolates exhibit distinct heterochromatin islands, which reduce expression of underlying genes, some of which confer resistance when mutated. Targeting synthetic heterochromatin to implicated loci confirms that resistance results from heterochromatin-mediated silencing. Our analyses reveal that epigenetic processes promote phenotypic plasticity, allowing wild-type cells to adapt to non-favorable environments without altering their genotype. In some isolates, subsequent or co-occurring gene amplification events augment resistance. Caffeine impacts two anti-silencing factors: Epe1 levels are downregulated, reducing its chromatin association; and Mst2 histone acetyltransferase expression switches to a shortened isoform. Thus, heterochromatin-dependent epimutant formation provides a bet-hedging strategy that allows cells to remain genetically wild-type but adapt transiently to external insults. Unstable caffeine-resistant isolates show cross-resistance to antifungal agents, suggesting that related heterochromatin-dependent processes may contribute to antifungal resistance in plant and human pathogenic fungi.

[*]Corresponding author: robin.allshire@ed.ac.uk.
[†]Present address: Centre for Genomic Regulation (CRG), The Barcelona Institute of Science and Technology, Barcelona 08003, Spain

Author contributions

S.T-G., P.N.C.B.A. and R.C.A. conceived the project. S.T-G. and P.N.C.B.A. performed preliminary studies. S.T-G. performed experiments and bioinformatics. M.S. designed *cup1-3xDSR* experiments and contributed to ChIP-seq and qChIP experiments. A.L.P. performed cytology, *cup1-TT* and eccDNA experiments. I.Y. constructed Epe1 and Mst2 strains and performed western analysis. S.A.W. generated Cup1 point mutants, Cup1-GFP strain and contributed to Epe1 and Mst2 experiments. S.T-G., A.L.P. and R.C.A. wrote the manuscript.

Competing interests

The authors declare no competing interests.

Additional information

Supplementary Information is available for this paper.
Correspondence and requests for materials should be addressed to Robin Allshire.
Reprints and permissions information is available at www.nature.com/reprints

Europe PMC Funders Author Manuscripts

H3K9me-heterochromatin can be copied by a read-write mechanism[4,5,8] and has been observed to arise stochastically at various loci, albeit only in the absence of key anti-silencing factors[9–13] or specific growth conditions[14]. We reasoned that if heterochromatin can redistribute in wild-type *S. pombe* cells, epimutations could be generated, allowing adaption to external insults. Unlike genetic mutants we predicted that such epimutants would be unstable, resulting in gradual loss of resistance following growth without the insult. We chose to use caffeine because deletion of genes with a variety of cellular roles confers caffeine resistance[15], thereby increasing the chance of obtaining epimutations. We also reasoned that unstable epimutants would occur more frequently at moderate caffeine concentrations that prevent most cells from growing (16 mM) rather than the higher stringency (20 mM) used in screens for genetic caffeine-resistant mutants[15].

As secondary events might occur upon prolonged growth on caffeine, we froze an aliquot of each isolate upon resistant colony formation and also froze consecutive aliquots of each isolate after continued growth on caffeine (Fig. 1a). This ‘time series’ permitted detection and separation of potential initiating and subsequent events. Colonies that grew after plating wild-type fission yeast (972 h^-) cells in 16 mM caffeine (+CAF) were picked. Following freezing, isolates were then successively propagated without caffeine (-CAF). Re-challenging isolates with caffeine revealed that 23% lost caffeine resistance after 14 days of non-selective growth (‘unstable resistant’, UR) whereas 13% remained caffeine resistant (‘stable resistant’, SR). 64% of isolates did not display a clear phenotype (‘unclear’) (Fig. 1b and Extended Data Fig. 1a-c). Deletion of *clr4*$^+$ (the sole *S. pombe* H3K9 methyltransferase[16,17]), but not a control locus, from resistant isolates resulted in loss of caffeine resistance in unstable, but not stable isolates (Fig. 1c and Extended Data Fig. 1d). Thus, caffeine resistance in unstable isolates requires heterochromatin.

Whole genome sequencing (WGS) of stable isolate SR-1 uncovered a mutation in *pap1*$^+$ responsible for the caffeine-resistant phenotype (Extended Data Fig. 1e)[18]. ChIP-seq for H3K9me2 on SR-1 revealed no changes in heterochromatin distribution. WGS of unstable isolates revealed no genetic changes in any sequence involved in either caffeine resistance or H3K9me2-mediated silencing, and 8 of 30 analyzed unstable isolates had no detectable genetic change compared to wild-type (Extended Data Fig. 2a-e and Supplementary Table 1).

H3K9me2 ChIP-seq on unstable isolates revealed altered heterochromatin distributions. UR-1 exhibited a new H3K9me2 island over the *hba1* locus, whereas UR-2-to-UR-6 exhibited H3K9me2 islands over the *ncRNA.394*, *ppr4*, *grt1, fio1* and *mbx2* loci, respectively (Fig. 2 and Supplementary Table 1). Deletion of *hba1*$^+$ confers caffeine resistance[19], suggesting that caffeine-induced heterochromatin islands may drive resistance by silencing underlying genes. Accordingly, RT-qPCR analysis revealed reduced expression of genes underlying the observed *hba1* heterochromatin island (Extended Data Fig. 2f).

The *ncRNA.394*, *ppr4*, *grt1, fio1* and *mbx2* loci have not previously been implicated in caffeine resistance. Interestingly, 24/30 unstable isolates exhibited a heterochromatin island over the *ncRNA.394* locus (Extended Data Fig. 3a, b and Supplementary Table 1), and

reduced underlying transcript levels (Extended Data Fig. 2f and 3c), suggesting that transcriptional silencing within these loci mediates caffeine resistance.

ncRNA.394 was previously identified as a heterochromatin island that gains H3K9me2 in the absence of counteracting Epe1 demethylase[9,20]. We detected no H3K9me2 over *ncRNA.394* in untreated wild-type cells (Fig. 2b and Extended Data Fig. 3a, b). Deletion of *ncRNA.394* did not result in caffeine resistance (Extended Data Fig. 3d). Prolonged growth without caffeine of cells exhibiting the *ncRNA.394* heterochromatin island resulted in H3K9me2 loss over this region, whereas growth with caffeine extended the H3K9me2 domain over the *SPBC17G9.13c*$^+$ and *SPBC17G9.12c*$^+$ genes (Extended Data Fig. 3e). Deletion of *SPBC17G9.12c*$^+$ or *eno101*$^+$ did not result in caffeine resistance (Extended Data Fig. 3d). *SPBC17G9.13c*$^+$ is essential for viability, precluding testing its deletion for resistance.

To test if heterochromatin formation at these specific loci alone results in caffeine resistance, *tetO* binding sites were inserted at *hba1*, *ncRNA.394* and *mbx2* loci to force synthetic heterochromatin assembly upon recruitment of TetR-Clr4* fusion protein[4,5]. Combining *tetO* with TetR-Clr4* without anhydrotetracycline (-AHT) resulted in novel H3K9me2 domains and growth on caffeine (Fig. 3 and Extended Data Fig. 4a-d). Thus, heterochromatin-mediated silencing at *hba1*, *ncRNA.394* or *mbx2* loci results in caffeine resistance.

Remarkably, strains with forced synthetic heterochromatin at either *hba1* or *ncRNA.394* loci displayed resistance to the widely-used antifungals clotrimazole, tebuconazole and fluconazole (Fig. 3 and Extended Data Fig. 4e). Unstable caffeine-resistant isolates with heterochromatin islands at *hba1* (UR-1) or *ncRNA.394* (UR-2) loci also displayed resistance to antifungals and produced small interfering RNAs (siRNAs) homologous to surrounding genes (Extended Data Fig. 5a-c). Consistent with RNAi pathway involvement, caffeine resistance was abolished upon removal of RNAi components (*dcr1Δ*, *ago1Δ*; Extended Data Fig. 5d).

TetR-Clr4* tethering close to *SPBC17G9.13c*$^+$, upstream of *ncRNA.394*, resulted in caffeine resistance (Fig. 3c), suggesting that reduced *SPBC17G9.13c*$^+$ expression may mediate resistance. We therefore reduced expression of *SPBC17G9.13c*$^+$ (named *cup1*$^+$, *caffeine unstable phenotype 1*) by increasing degradation of its mRNA (*LocusPX:cup1-3xDSR*) or attenuating its transcription (*cup1-TT*; see Methods). Both approaches resulted in reduced *cup1*$^+$ transcript levels and caffeine resistance (Extended Data Fig. 6a, b). Cup1 contains a LYR domain often found in mitochondrial proteins[21] and Cup1-GFP exhibited mitochondrial localisation (Extended Data Fig. 6c). LYR-domain mutation led to caffeine resistance (Extended Data Fig. 6d). Thus, reduced expression or mutation of mitochondrial protein Cup1 (SPBC17G9.13c) renders cells caffeine resistant. We conclude that *cup1*$^+$ silencing by heterochromatin island formation mediates caffeine resistance.

In addition to the *ncRNA.394/cup1* heterochromatin island, analysis of ChIP-seq input DNA indicated that many independent unstable caffeine-resistant isolates also contained increased

copy number of a chromosome III region (Extended Data Fig. 7a). The minimal region of overlap in 11/12 isolates contained *cds1*$^+$, whose overexpression confers caffeine resistance[22]. To determine if *cds1*$^+$ amplification occurred before or after *ncRNA.394/cup1* heterochromatin island formation, we analyzed UR-2 samples frozen at earlier and later time points. The *ncRNA.394/cup1* H3K9me2 island was detected in the initial caffeine-resistant isolate (4day/+CAF), whereas *cds1* locus amplification arose later (7day/+CAF) (Extended Data Fig. 7b). Thus, development of resistance appears to be a multistep process where combinatorial events facilitate adaption to the insult.

In agreement with this hypothesis, deletion of *clr4*$^+$ from the initial UR-2 isolate (4day/+CAF) resulted in caffeine resistance loss in all transformants (6/6). However, only half of the transformants (3/6; transformants 1, 4 and 5) lost caffeine resistance upon *clr4*$^+$ deletion from the later UR-2 isolate with *cds1* locus amplification (7day/+CAF). Transformants that retained resistance after *clr4*$^+$ removal (3/6; transformants 2, 3 and 6) exhibited higher *cds1*$^+$ copy numbers compared to *clr4Δ* transformants that lost resistance or to wild-type cells (Extended Data Fig. 7c). We conclude that once *cds1* locus amplification occurs heterochromatin is no longer required for caffeine resistance. In UR-2 the new *ncRNA.394/cup1* heterochromatin island arose before *cds1*$^+$ amplification, but it is likely that these events are stochastic and occur in no fixed order. Interestingly, both adaptations – island formation and locus amplification – are unstable and lost following growth without caffeine (Extended Data Fig. 7d).

Instability of the amplified region suggested it resulted from excision and extrachromosomal circular DNA (eccDNA) formation which can be rapidly accumulated and lost[23–26]. CNV plots revealed repetitive elements at junctions of putative eccDNA (*5S rRNA.24/26* for UR-2 (7day/+CAF) and *LTR3/27* for UR-4). PCR specific for putative circle junctions and Southern analysis confirmed the presence of chromosome-III-derived eccDNA (Extended Data Fig. 8). Therefore, repeat-mediated eccDNA generation provides an alternative, or supplementary, mechanism for the evolution of caffeine, and perhaps other, resistances in fission yeast. Accumulation of additional changes may allow further adaption to insults through other pathways or by bolstering silencing at particular loci[27].

To investigate the dynamics of heterochromatin island formation in response to caffeine we exposed wild-type cells to low (7 mM) or medium (14 mM) doses of caffeine. Cells in low or medium caffeine doubled ~8 or ~3 times, respectively, in 18 hours (Extended Data Fig. 9a). Several H3K9me2 heterochromatin islands were detected following exposure to low caffeine (Fig. 4a top and Extended Data Fig. 9b, c). These low-caffeine-induced islands represent a subgroup of those that accumulate H3K9me2 in the absence of Epe1[9,10,12], including *ncRNA.394/cup1*, but did not overlap with H3K9me2-heterochromatin domains that accumulate without nuclear exosome function[13] or at 18°C[14]. Remarkably, ectopic heterochromatin was restricted to *ncRNA.394/cup1* following medium caffeine treatment and H3K9me2 levels at this locus were ~4-fold greater after medium compared to low caffeine exposure (Fig. 4a and Extended Data Fig. 9d). These data indicate that exposure to near-lethal doses of caffeine (14 mM) allows wild-type cells to develop resistance rapidly by forming heterochromatin over a locus (*ncRNA.394/cup1*) that confers resistance when silenced.

To determine if other insults also induce heterochromatin islands, we exposed wild-type cells to oxidative stress (1 mM hydrogen peroxide). Heterochromatin islands were detected at similar locations to those observed in low caffeine, albeit H3K9me2 levels were lower (Extended Data Fig. 9b, c and e).

The heterochromatin profile of wild-type cells treated with low caffeine resembles that of untreated *epe1Δ* cells (Extended Data Fig. 9c). We hypothesized that caffeine might negatively regulate Epe1, thereby allowing adaptive ectopic heterochromatin islands to form in wild-type cells. TetR-Clr4*-mediated synthetic heterochromatin can be transmitted through cell division upon release of TetR-Clr4* from *tetO* sites only in cells lacking Epe1[4,5]. To further test if caffeine imparts an *epe1Δ*-like phenotype, we treated wild-type cells with low caffeine and released TetR-Clr4* from *4xtetO* sites inserted at *ura4*$^+$ (Fig. 4b). Caffeine treatment, like *epe1Δ*, allowed heterochromatin retention at the tethering site for longer compared to untreated cells. *epe1*$^+$ RNA levels were not significantly altered by caffeine, suggesting post-transcriptional regulation (Extended Data Fig. 9f). 3xFLAG-Epe1 levels decreased by 33% and Epe1 association with various heterochromatic locations was reduced following exposure to caffeine (Fig. 4c, d). These data suggest that down-regulation of Epe1 putative H3K9 demethylase levels plays a critical role in the response to external insults by allowing formation of adaptive ectopic H3K9me-heterochromatin islands that, in turn, reduce expression of underlying genes to confer resistance. Consistent with this scenario, *epe1Δ* cells form more, and *clr4Δ* cells fewer, caffeine resistant colonies than wild-type cells (Extended Data Fig. 9g).

Although caffeine down-regulates Epe1 protein levels, higher levels of H3K9me2 accumulate at heterochromatin islands following caffeine exposure than in untreated *epe1Δ* cells (Extended Data Fig. 9c). Therefore, reduced Epe1 levels alone cannot account for the high levels of H3K9me2 observed at islands upon caffeine treatment. Mst2 histone acetyltransferase acts synergistically with Epe1 to prevent heterochromatin island formation[10]. Interestingly, caffeine exposure results in production of a shorter Mst2 protein by wild-type cells (52 kDa versus 62 kDa; Extended Data Fig. 10a). RNA-seq suggests this shorter isoform arises through use of an alternative transcriptional start site in caffeine, such as that detected in other stresses[28] (Extended Data Fig. 10b). We suggest that this caffeine-induced shortened Mst2 isoform, lacking the MYST-Zinc finger domain[29], may be inactive and unable to prevent heterochromatin island formation. Thus, caffeine, by both lowering Epe1 levels and likely disabling Mst2, allows greater accumulation of H3K9me2 at islands than in *epe1Δ* cells. These findings reveal an adaptive epigenetic response to external insults that stimulates phenotypic plasticity, and suggest that stress-response pathways may regulate heterochromatin modulation activities, thereby ensuring cell survival in fluctuating environmental conditions (Fig. 4e).

DNA methylation-dependent epimutations frequently arise in plants and are propagated by maintenance methyltransferases[30,31]. RNAi-mediated epimutations occur in the fungus *Mucor circinelloides* [32], but their DNA methylation or heterochromatin dependence is unknown. As fission yeast lacks DNA methylation[33,34] this epigenetic mark cannot be responsible for the epimutations described here. Instead our analyses indicate that these

adaptive epimutations are transmitted in wild-type cells by the Clr4/H3K9me read-write mechanism[4,5,8].

Why have epimutants not been detected previously in mutant screens? Stringent phenotypic screens mean strong mutants are investigated further and eccentric mutants discarded. Here we selected for weak mutants by applying sublethal doses of drug at the threshold of growth prevention. Selection was time-limited to maximize identification of isolates exhibiting unstable phenotypes prior to development of genetic alterations.

Fungal infections are on the rise, especially in immunocompromised humans. Few effective antifungal agents exist and resistance is rendering them increasingly ineffective[35]. Widespread use of related azole compounds to control fungus-mediated crop deterioration may leave residual antifungals in the soil, possibly allowing unwitting selection of resistant epimutants in fungi, ultimately driving increasing cases of azole-resistant Aspergillosis and Cryptococcosis in the clinic. Monitoring resistance in clinical isolates involves mutation identification by genome sequencing, but resistance due to epimutations – similar to those described here – would be missed, leading to inaccurate diagnoses. Re-engineering existing so-called ‘epigenetic drugs’ – compounds that inhibit histone-modifying enzymes – or development of novel agents, may identify molecules that specifically block fungal, not host, heterochromatin formation, hence reducing the emergence of antifungal resistance in clinical and agricultural settings.

Methods

Yeast strains and manipulations

Standard methods were used for fission yeast growth, genetics and manipulation[36]. *S. pombe* strains used in this study are described in Supplementary Table 2. Oligonucleotide sequences are listed in Supplementary Table 3. For pDUAL-adh21-TetR-2xFLAG-Clr4-CDΔ (abbreviated as TetR-Clr4*), the *nmt81* promoter of pDUAL-nmt81-TetR-2xFLAG-Clr4-CDΔ[4], was replaced by the *adh21* promoter (pRAD21, gift from Y. Watanabe). *Not*I-digested plasmid was integrated at *leu1*$^+$.

To reduce expression of *SPBC17G9.13c*$^+$/*cup1*$^+$ we used two independent strategies. First, we expressed an additional copy of *cup1*$^+$ with three nuclear exosome RNA degradation motifs (DSR; Determinant of Selective Removal[37,38]) fused to its 3’ untranslated region from an intergenic locus (*LocusPX:cup1-3xDSR*). Following insertion of *cup1-3xDSR* at *LocusPX*, endogenous *cup1*$^+$ was deleted and cells expressing only *cup1-3xDSR* were analysed. Second, the 144-bp transcriptional terminator site from *ura4*$^+$ was inserted in place of part of the putative *cup1*$^+$ promoter (*cup1-TT*) and cells were analysed.

pap1-N424STOP, *clr5-Q264STOP meu27-S100Y*, *LocusPX:cup1-3xDSR*, *cup1-TT*, *cup1-L73G*, *cup1-F99G*, *cup1-GFP, 3xFLAG-epe1* and strains carrying *4xtetO* insertions were constructed by CRISPR/Cas9-mediated genome editing using the *SpEDIT* system (Allshire Lab; available on request) with oligonucleotides listed in Supplementary Table 3. The mitochondrial protein Arg11[39], Epe1 and Mst2 were C-terminally tagged with mCherry (Arg11), GFP (Epe1) or 13xMyc (Mst2) using the Bähler tagging method[40].

Yeast extract plus supplements (YES) was used to grow all cultures. 16 mM caffeine (Sigma, C0750) was added to media for caffeine resistance screens and serial dilution assays. To screen for unstable caffeine-resistant isolates, caffeine-resistant colonies that formed seven days after plating wild-type cells on 16 mM caffeine YES (+CAF) plates were picked and patched to +CAF plates. After four days of growth, isolates were frozen (4day/+CAF). 4day/+CAF isolates were re-patched and grown for three days on +CAF plates and then frozen (7day/+CAF). Subsequently, 7day/+CAF isolates were re-patched every three days on +CAF plates up to twenty days of total growth on +CAF plates and then frozen (20day/+CAF).

0.29 μM clotrimazole (Sigma, C6019) was added to media for clotrimazole resistance serial dilution assays. 1.6 μM tebuconazole (Sigma, 32013) was added to media for tebuconazole resistance serial dilution assays. 0.6 mM fluconazole (Sigma, PHR1160) was added to media for fluconazole resistance serial dilution assays.

7 or 14 mM caffeine (Sigma, C0750), or 1 mM hydrogen peroxide (Sigma, H1009) were added to media for 18 hours for drug treatment experiments. To release *TetR-Clr4**, 10 μM anhydrotetracycline (AHT) was added to the media.

Serial dilution assays

Equal amounts of starting cells were serially diluted five-fold and then spotted onto appropriate media. Cells were grown at 30-32°C for 3-5 days and then photographed.

Chromatin immunoprecipitation (ChIP)

ChIP experiments were performed as previously described[41] using anti-H3K9me2 (5.1.1, gift from Takeshi Urano) or anti-GFP (Invitrogen, A11122). Immunoprecipitated DNA was recovered with Chelex-100 resin (BioRad) for ChIP-qPCR (qChIP) experiments or with QIAquick PCR Purification Kit (Qiagen) for ChIP-seq experiments.

Quantitative ChIP-qPCR (qChIP)

qChIPs were analysed by real-time PCR using Lightcycler 480 SYBR Green (Roche) with oligonucleotides listed in Supplementary Table 3. All ChIP enrichments were calculated as % DNA immunoprecipitated at the locus of interest relative to the corresponding input samples and normalized to % DNA immunoprecipitated at the *act1* $^{+}$ locus. For spike-in qChIPs, an equal number (~20%) of *Schizosaccharomyces octosporus* cells (H3K9me2 spike-in qChIP)[41] or Sgo1-GFP *Saccharomyces cerevisiae* cells (GFP spike-in qChIP)[42] (gift from Adele Marston) were added to initial *S. pombe* pellets. Histograms represent data averaged over three biological replicates. Error bars represent standard deviations.

ChIP-seq library preparation and analysis

Illumina-compatible libraries were prepared as previously described[41] using NEXTflex-96 barcode adapters (Bioo Scientific) and Ampure XP beads (Beckman Coulter). Libraries were then pooled to allow multiplexing and sequenced on an Illumina HiSeq2000, NextSeq or MiniSeq system (150-cycle high output kit) by 75 bp paired-end sequencing.

Approximately 6-10 million 75 bp paired-end reads were produced for each sample. Raw reads were then de-multiplexed and trimmed using Trimmomatic (v0.35)[43] to remove adapter contamination and regions of poor sequencing quality. Trimmed reads were aligned to the *S. pombe* reference genome (*972h*$^-$, ASM294v2.20) using Bowtie2 (v2.3.3)[44]. Resulting bam files were processed using Samtools (v1.3.1)[45] and picard-tools (v2.1.0) (http://broadinstitute.github.io/picard) for sorting, removing duplicates and indexing. Coverage bigwig files were generated by BamCoverage (deepTools v2.0) and ratios IP/input were calculated using BamCompare (deepTools v2.0)[46] in SES mode for normalisation[47]. Peaks were called using MACS2[48] in PE mode and broad peak calling (broad-cutoff = 0.05). Region-specific H3K9me2 enrichment plots were generated using the Sushi R package (v1.22)[49]. Heatmaps were generated using computeMatrix and plotHeatmap (deepTools v2.0)[46] with genomic coordinates indicated in Supplementary Table 4.

SNP and indel calling

SNPs and indels were called as previously described[50]. Trimmed reads were mapped to the *S. pombe* reference genome (*972h*$^-$, ASM294v2.20) using Bowtie2 (v2.3.3)[44]. GATK[51,52] was used for base quality score recalibration. SNPs and indels were called with GATK HaplotypeCaller[51,52] and filtered using custom parameters. Functional effect of variants was determined using Variant Effect Predictor[53].

Copy number variation analysis

Copy number variation was determined using CNVkit[54] in Whole-Genome Sequencing (-wgs) mode. Wild-type ChIP-seq input bam files were used as reference.

Extrachromosomal circular DNA diagnostic PCRs and Southern analysis

ChIP-input DNA samples were used as template for PCR with Taq polymerase (Roche, 4728858001) according to manufacturer's instructions. Two types of PCR were performed: control PCR for loci present on endogenous chromosome III (expected to be present in wild-type, UR-2 (7day/+CAF) and UR-4) and circle-specific PCRs specific for putative extrachromosomal circles predicted to be present in UR-2 (7day/+CAF) or UR-4. For wild-type and UR-2 (7day/+CAF): control primers were located on either on side of *5S rRNA.24* (primers A (forward), B (reverse); see Supplementary Table 3) and *5S rRNA.26* (primers C, D); circle-specific primers were located on either side of a predicted junction between *5S rRNA.24* and *5S rRNA.26* (primers C and B). For wild-type and UR-4: control primers were located on either on side of *LTR3* (primers E, F) and or *LTR27* (primers G, H); circle-specific primers were located on either side of a predicted junction between *LTR3* and *LTR27* (primers G and F). For some locations, more than one forward and/or reverse primer was used, for instance: forward primers C1, C2 with reverse primers D1, D2. PCR products were electrophoresed on 2% agarose gels containing Ethidium Bromide.

For Southern analysis, genomic DNA was prepared from wild-type, UR-2 (7day/+CAF) and UR-4 cultures grown in YES. Briefly, cells were incubated with Zymolyase 100T (AMS Biotechnology) to digest the cell wall, pelleted, resuspended in TE and lysed with SDS, followed by addition of potassium acetate and precipitation with isopropanol. After treatment with RNase A and proteinase K, phenol chloroform and chloroform extractions

were performed. DNA was precipitated in the presence of sodium acetate and ethanol, followed by centrifugation and washing of the pellet with 70% ethanol. After air drying the pellet was resuspended in TE. Approximately 8 μg of DNA was digested with the following restriction enzymes: wild-type and UR-2 (7day/+CAF): *Bsm*BI, *Eco*RV, *Nde*I; wild-type and UR-4: *Eco*RI, *Bam*HI + *Xba*I. Digested DNA was subjected to electrophoresis in a 0.9 % agarose gel containing ethidium bromide. Southern blotting was achieved by the alkali transfer method. Briefly, the gel was depurinated with 0.3 M HCl for 10 minutes, washed with distilled water, followed by two 15 min incubations in Denaturing Solution (0.5 M NaOH, 1.5 M NaCl). Overnight capillary transfer was used for transfer to Hybond XL membrane (Amersham), which was then washed with 50 mM Na_2HPO_4 pH7.2, followed by air drying. After drying at 80°C for 2 hours and UV-crosslinking, membranes were prehybridized in Church Buffer (0.5 M Na_2HPO_4 pH 7.2, 7% SDS, 1 mM EDTA, 1% BSA (Sigma, A0281) for 1 hour at 65°C. Probes were made using High Prime kit (Roche, 11585592001) and α-^{32}P-dCTP (NEN), according to the manufacturer's instructions. Heat denatured probes in Church Buffer were hybridized with relevant membranes at 65°C overnight with rotation. Following washes with Wash Buffer (40 mM Na_2HPO_4 pH 7.2, 1 mM EDTA, 1% SDS) blots were exposed to XAR-5 film (Kodak) at -80°C with an intensifying screen for several hours.

Cytology

Schizosaccharomyces pombe cultures were fixed before processing for immunofluorescence as described[41]. Briefly, cells in YES culture were fixed with 3.7% formaldehyde (Sigma, F8775) for 30 min, followed by cell wall digestion with Zymolyase-100T (AMS Biotechnology) in PEMS buffer (100 mM PIPES pH 7, 1 mM EDTA, 1 mM $MgCl_2$, 1.2 M Sorbitol). After permeabilization with Triton-X100, cells were washed, blocked in PEMBAL (PEM containing 1% BSA, 0.1% sodium azide, 100 mM lysine hydrochloride). Rabbit anti-GFP (Invitrogen, A11122) was used in PEMBAL at 1:500 dilution, and Alexa 488-coupled chicken-anti-rabbit secondary antibody (Invitrogen, A21441) at 1:1000 dilution. Arg11-mCherry fluorescence survived fixation and no antibodies were used for localisation. Cells were stained with DAPI and mounted in Vectashield. Microscopy was performed with a Zeiss Imaging 2 microscope (Zeiss) using a 100x 1.4NA Plan-Apochromat objective, Prior filter wheel, illumination by HBO100 mercury bulb. Image acquisition with a Photometrics Prime sCMOS camera (Photometrics, https://www.photometrics.com) was controlled using Metamorph software (Version 7; Universal Imaging Corporation). Exposures were 3000 ms for FITC/Alexa-488 channel (Cup1-GFP/Alexa 488), 500 ms for TRITC channel (Arg11-mCherry) and 100 ms for DAPI. For display of images, maximum intensity was determined for e.g. Cup1-GFP staining in Cup1-GFP Arg11-mCherry strain (B4909) and this maximum was applied for scaling of all B4909 and B4912 (expresses only Arg11-mCherry) images. FITC and TRITC channels were scaled in this way; DAPI images were autoscaled.

qRT–PCR analysis

Total RNA was extracted using the Monarch Total RNA Miniprep Kit (New England Biolabs) according to the manufacturer's instructions. Contaminating DNA was removed by treating with Turbo DNase (Invitrogen) and reverse transcription was performed using LunaScript RT Supermix Kit (New England Biolabs). Oligonucleotides used for qRT-PCR

are listed in Supplementary Table 3. qRT-PCR histograms represent three biological replicates; error bars correspond to the standard deviation.

RNA-seq library preparation and analysis

Total RNA was extracted using the Monarch Total RNA Miniprep Kit (New England Biolabs) according to the manufacturer's instructions. Contaminating DNA was removed by treating with Turbo DNase (Invitrogen). rRNA was removed using the Ribo-Zero Gold rRNA removal kit (Yeast) (Illumina) before library construction using NEBNext Ultra II Directional RNA Library Prep Kit for Illumina (New England Biolabs). Libraries were pooled and sequenced on an Illumina NextSeq platform by 75 bp paired-end sequencing. Adapter-trimmed reads were aligned to the *S. pombe* reference genome (*972h*$^{-}$, ASM294v2.20) using STAR (v2.2.1)[55] and processed using Samtools (v1.3.1)[45]. Coverage bigwig files were generated by BamCoverage (deepTools v2.0)[46].

Differential expression was analysed using the Bioconductor Rsamtools (v2.0.3), GenomicFeatures (v1.36.4)[56] and DESeq2 (v.1.24)[57] R libraries. Log2 fold changes were shrunk using the apeglm method[58] and a MA-plot was generated using R. Genes with an adjusted *p* value below 0.01 are shown in red.

Small RNA-seq

50 mL of log-phase cells were collected and processed using the mirVana miRNA Isolation kit (Invitrogen). Resulting sRNA was treated with TURBO DNase (Invitrogen) and used for library construction using NEBNext Multiplex Small RNA Library Prep Set for Illumina (New England Biolabs) according to manufacturer's instructions. Libraries were pooled and sequenced on an Illumina NextSeq platform by 50 bp single-end sequencing. Raw reads were then de-multiplexed and processed using Cutadapt (v1.17) to remove adapter contamination and discard reads shorter than 19 nucleotides or longer than 25 nucleotides. Coverage plots were generated using SCRAM[59].

Protein extraction and western analysis

Protein samples were prepared as previously detailed[60]. Western blotting detection was performed using anti-FLAG-HRP (Sigma, A8591), anti-Myc (Cell Signalling, 9B11), anti-a-tubulin (gift from Keith Gull)[61], goat anti-mouse (Sigma, A4416), anti-Bip1[62], goat anti-rabbit (Sigma, A6154), anti-Cdc11 (gift from Ken Sawin) and donkey anti-sheep (Abcam, ab6900). Gels were visualised using the ChemiDoc imaging system (BioRad) and analysed with ImageJ.

Extended Data

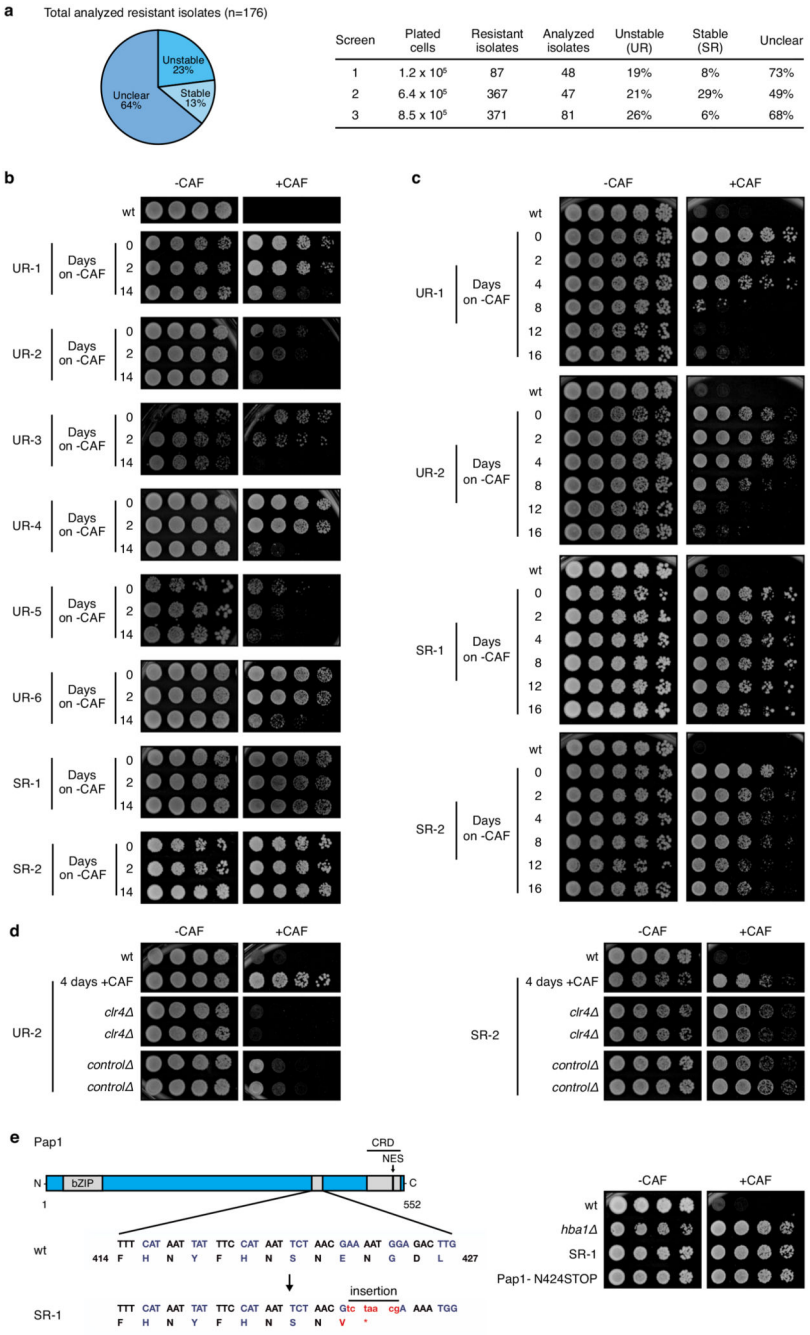

Extended Data Figure 1. Identification of heterochromatin-dependent epimutants resistant to caffeine

a, Frequency of unstable (UR) and stable (SR) caffeine-resistant isolates obtained from 3 independent screens. 64% of isolates did not display a clear phenotype (unclear).

b, Unstable (UR) and stable (SR) caffeine-resistant isolates were identified using this screening strategy. After growth on non-selective media for 14 days caffeine resistance is lost in UR isolates but not in SR isolates.

c, Caffeine resistance is lost progressively in unstable (UR) isolates but maintained in stable (SR) isolates.

d, Caffeine resistance in UR isolates depends on the Clr4 H3K9 methyltransferase. *clr4*$^{+}$ (*clr4Δ*) or an unlinked intergenic region (*control Δ*) were deleted in unstable (UR-2) and stable (SR-2) caffeine-resistant isolates.

e, A mutation in *pap1*$^{+}$ confers caffeine resistance in the stable isolate SR-1. *Left*: Whole genome sequencing of the stable isolate SR-1 revealed a 7-nucleotide insertion in *pap1*$^{+}$. The insertion results in a truncated Pap1 protein (Pap1-N424STOP) that lacks the Nuclear Export Signal (NES). CRD: Cysteine-rich domain. *Right*: Pap1-N424STOP is resistant to caffeine. The 7-nucleotide insertion identified in SR-1 was introduced into the *pap1*$^{+}$ gene of wild-type cells (Pap1-N424STOP) and caffeine resistance assessed. *hba1Δ* and SR-1 cells were used as positive controls.

Experiments in (**b-d**) and (**e,** *right*) were independently repeated at least twice with similar results.

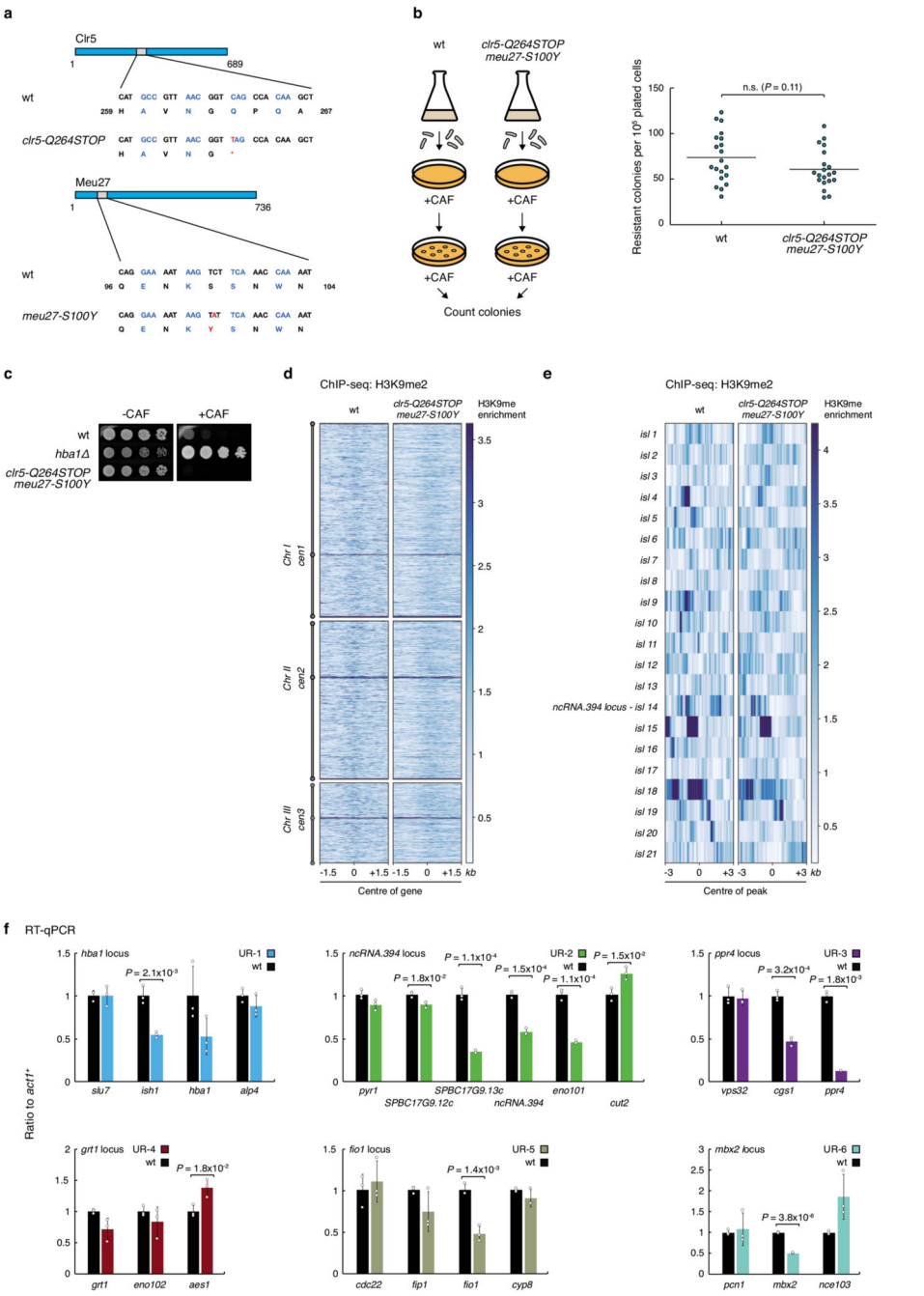

Extended Data Figure 2. Unstable (UR) caffeine-resistant isolates are *bona fide* epimutants.

a-e, Genetic changes (*clr5-Q264STOP meu27-S100Y*) found in 4 of 30 unstable isolates do not contribute to the caffeine-resistant phenotype nor cause the formation of ectopic heterochromatin.

a, Whole genome sequencing of unstable isolates UR-1/3/5/7 revealed a Single Nucleotide Polymorphism (SNP) in *clr5*$^{+}$ (*clr5-Q264STOP*) and in *meu27*$^{+}$ (*meu27-S100Y*).

b, *Left*: Schematic of experiment to determine whether *clr5-Q264STOP meu27-S100Y* cells form more caffeine-resistant colonies than wild-type cells. Wild-type (wt) and *clr5-*

Europe PMC Funders Author Manuscripts

Europe PMC Funders Author Manuscripts

Q264STOP meu27-S100Y cells were plated on +CAF media (10^5 cells per plate, 20 plates per strain). Caffeine-resistant colonies were counted after 7 days. *Right*: *clr5-Q264STOP meu27-S100Y* form a similar number of caffeine-resistant colonies to wt cells. Data are mean from twenty technical replicates. *P* value from a two-tailed Student's *t*-test is indicated.

c, *clr5-Q264STOP meu27-S100Y* cells are not resistant to caffeine. *clr5-Q264STOP meu27-S100Y* cells were serially diluted and spotted on -CAF and +CAF plates to assess caffeine resistance. *hba1Δ* cells served as a positive control. Experiment was independently repeated at least twice with similar results.

d, Genome-wide H3K9me2 ChIP-seq enrichment in wt and *clr5-Q264STOP meu27-S100Y* cells. Data are represented as relative fold enrichment over input.

e, H3K9me2 ChIP-seq enrichment at known heterochromatin islands detected in *epe1Δ* cells[9] in wt and *clr5-Q264STOP meu27-S100Y* cells. Data are represented as relative fold enrichment over input.

f, Gene transcript levels within and flanking ectopic heterochromatin islands in individual isolates. See Figure 2b. Data are mean ± s.d. from three biological replicates. *P* values < 0.05 from a two-tailed Student's *t*-test are indicated.

Europe PMC Funders Author Manuscripts

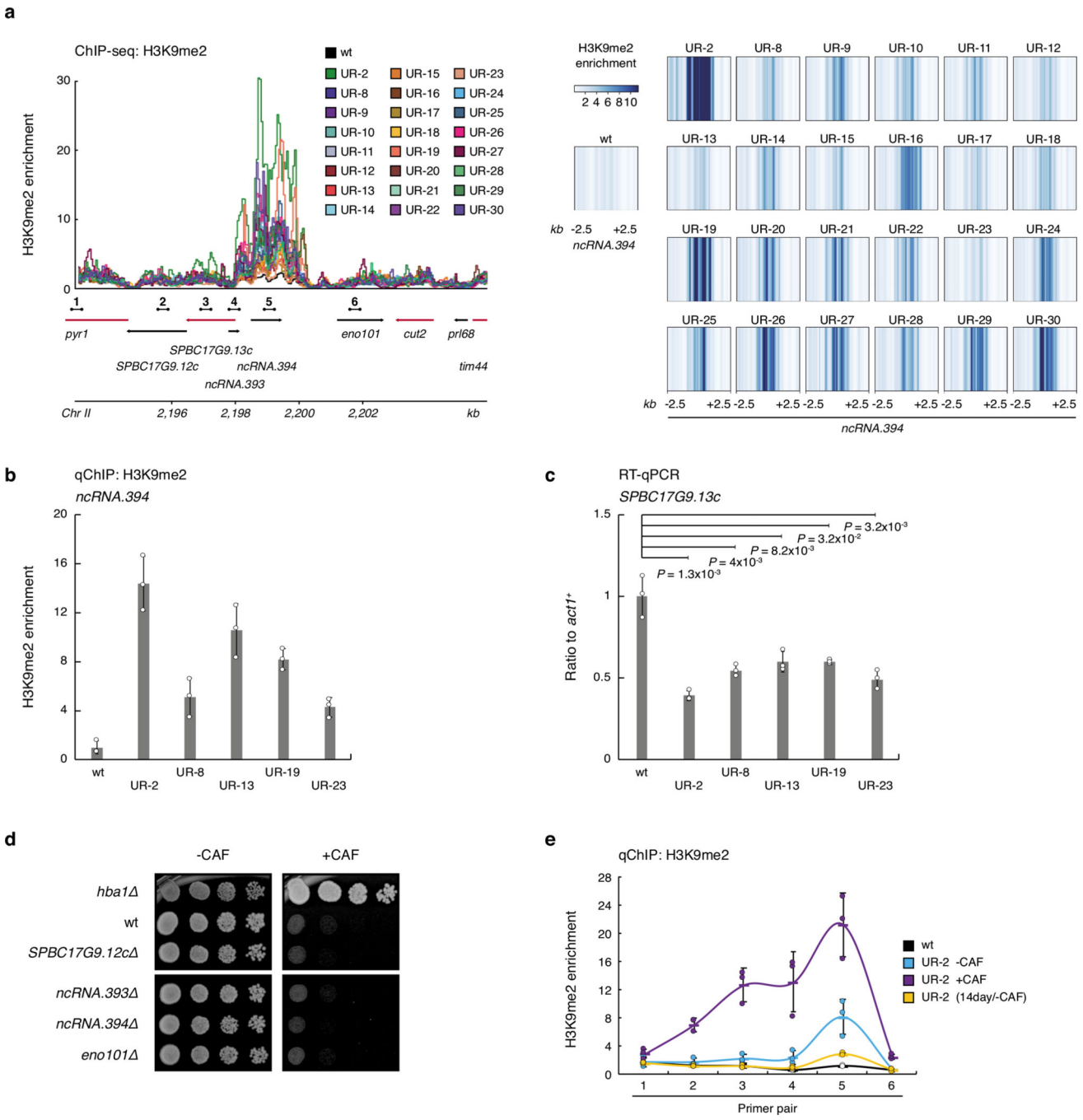

Extended Data Figure 3. 24 of 30 unstable (UR) caffeine-resistant isolates display an ectopic heterochromatin island over the *ncRNA.394* locus

a, H3K9me2 ChIP-seq enrichment at the *ncRNA.394* locus in individual isolates (*left*: coverage tracks; *right*: heatmaps). Data are represented as relative fold enrichment over input. Relevant genes within and flanking ectopic heterochromatin islands are indicated. Red arrows indicate essential genes. Dumbbells indicate primer pairs used in **b, c** and **e**.

b, Quantitative chromatin immunoprecipitation (qChIP) of H3K9me2 levels on *ncRNA.394* in individual isolates. Data are mean ± s.d. from three biological replicates. Primer pairs used are indicated in **a** (*ncRNA.394*, primer pair 5).
c, *SPBC17G9.13c*$^{+}$ gene transcript levels in individual isolates. Data are mean ± s.d. from three biological replicates. *P* values from a two-tailed Student's *t*-test are indicated. Primer pairs used are indicated in **a** (*SPBC17G9.13c*$^{+}$, primer pair 3).
d, Deletion of *ncRNA.394* or non-essential adjacent genes does not result in caffeine resistance. Experiment was independently repeated at least twice with similar results.
e, qChIP of H3K9me2 levels at the *ncRNA.394* locus in UR-2 cells. UR-2 cells were grown in the absence (-CAF) or presence (+CAF) of caffeine overnight or in the absence of caffeine for 14 days (+14day/-CAF). Data are mean ± s.d. from three biological replicates. Primer pairs used are indicated in **a**.

Europe PMC Funders Author Manuscripts

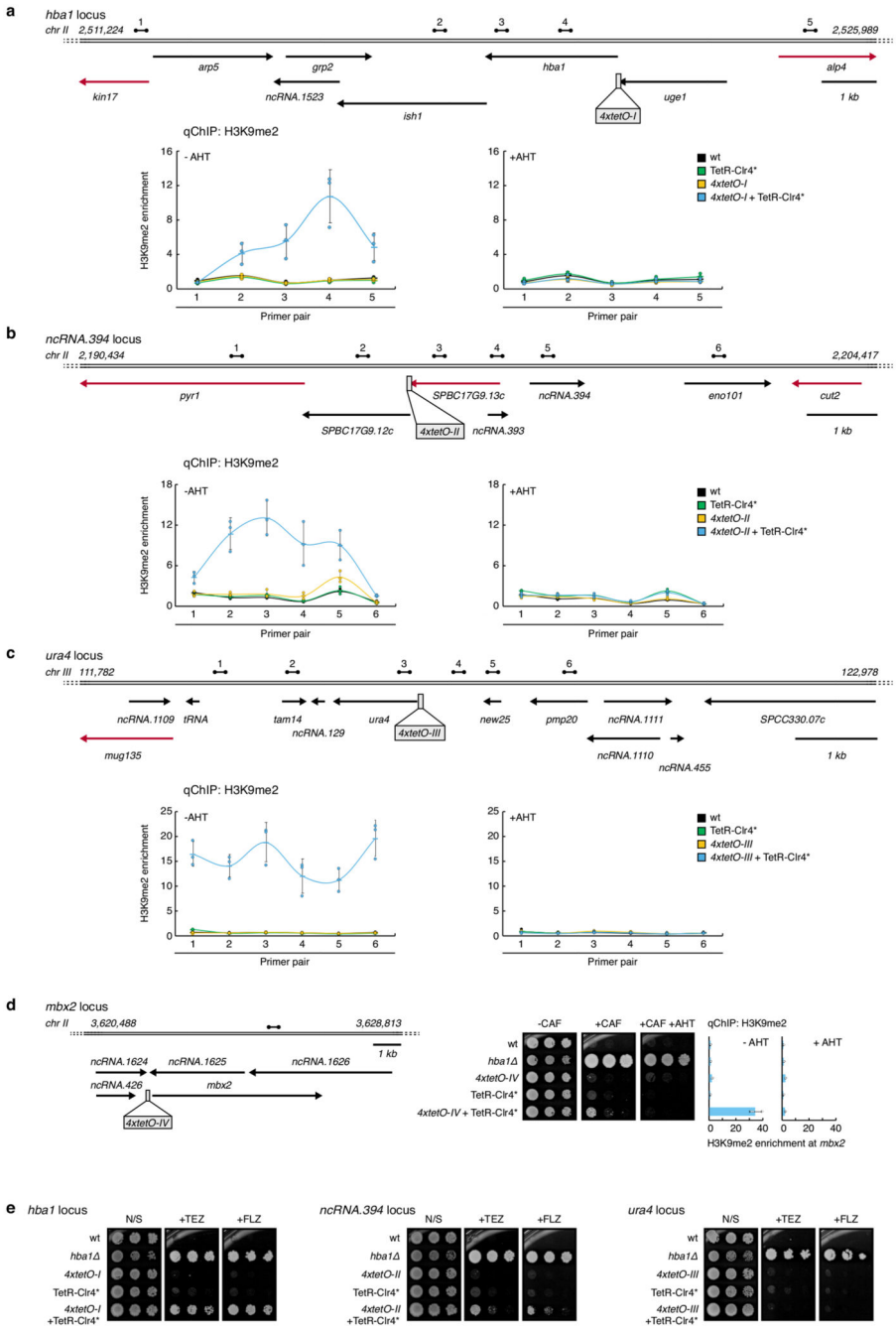

Extended Data Figure 4. Forced synthetic heterochromatin targeting to the identified loci is sufficient to drive caffeine resistance in wild-type cells

a-c, Quantitative chromatin immunoprecipitation (qChIP) of H3K9me2 levels in wild-type (wt) cells harbouring *4xtetO* binding sites at the identified ectopic heterochromatin loci (or *ura4* as control) and expressing TetR-Clr4* in the absence or presence of AHT. **a,** *hba1* locus. **b,** *ncRNA.394* locus. **c,** *ura4* locus. Data are mean ± s.d. from three biological replicates. Dumbbells indicate primer pairs used. Red arrows indicate essential genes.

Europe PMC Funders Author Manuscripts

d, Forced synthetic heterochromatin targeting to the *mbx2* locus is sufficient to drive caffeine resistance in wt cells. qChIP of H3K9me2 levels in wt cells harbouring *4xtetO* binding sites at the *mbx2* ectopic heterochromatin locus and expressing TetR-Clr4* in the absence or presence of AHT. Data are mean ± s.d. from three biological replicates. Dumbbells indicate primer pairs used.

e, Strains from **a-c** were assessed for resistance to the antifungal agents tebuconazole (+TEZ) and fluconazole (+FLZ). Experiments were independently repeated at least twice with similar results.

Europe PMC Funders Author Manuscripts

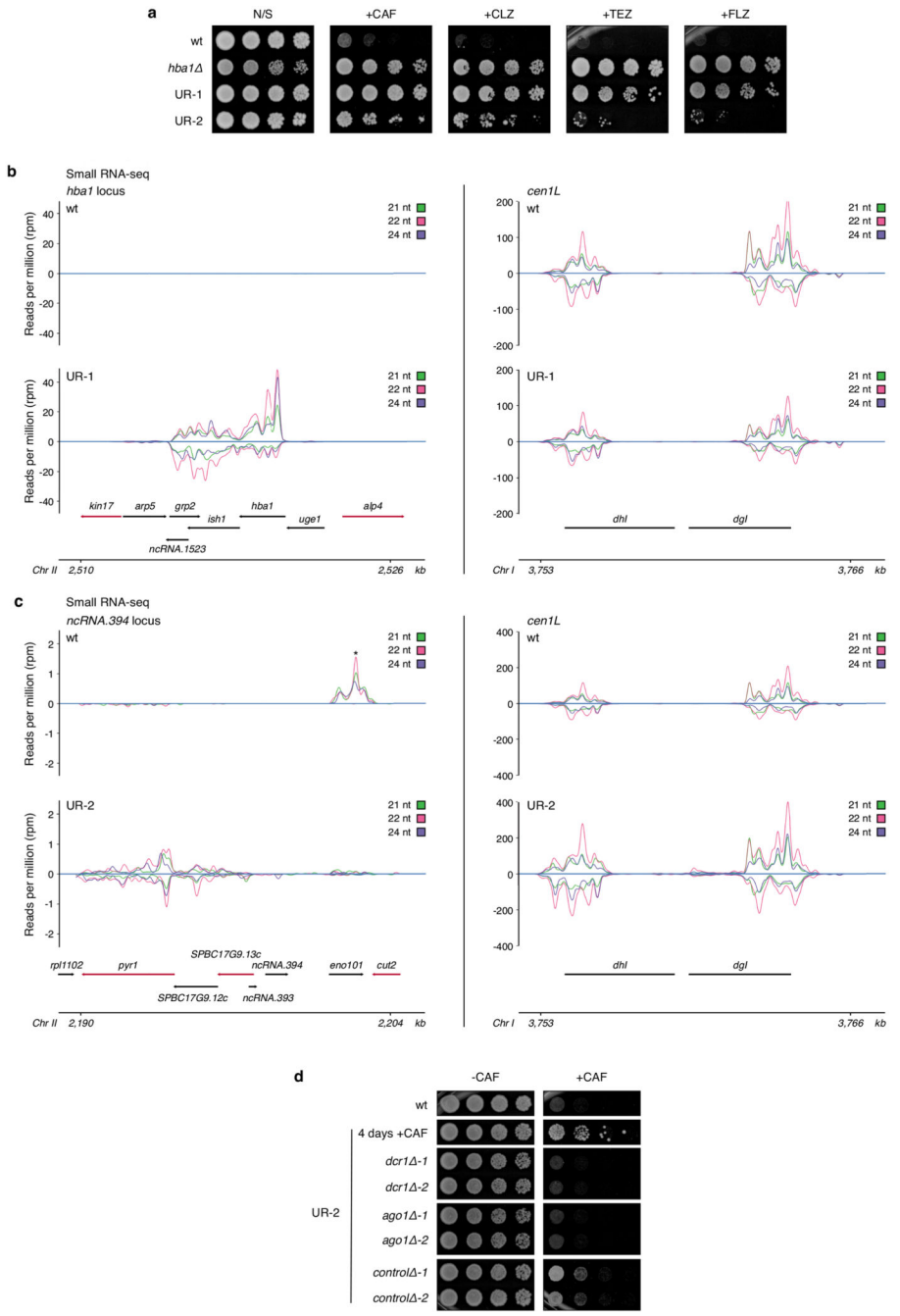

Extended Data Figure 5. Unstable (UR) caffeine-resistant isolates show cross-resistance to antifungals and siRNA generation at ectopic heterochromatin islands

a, Unstable caffeine-resistant isolates UR-1 and UR-2 were serially diluted and spotted on non-selective (N/S), caffeine (+CAF), clotrimazole (+CLZ), tebuconazole (+TEZ) and fluconazole (+FLZ) media to assess resistance. Experiment was independently repeated at least twice with similar results.

b-c, *Left*: small RNA sequencing detects siRNAs (21-24 nucleotides) homologous to ectopic heterochromatin islands in UR-1 (**b**, *hba1 locus*) and UR-2 (**c**, *ncRNA.394* locus) compared

Europe PMC Funders Author Manuscripts

to wild-type (wt) cells. *Right*: siRNAs mapping to pericentromeric *dgI/dhI* repeats of chromosome I shown as control. Sequencing was performed once. *Transcripts mapping to the highly-expressed gene *eno101*$^{+}$ in euchromatic wild-type conditions (note these are unidirectional RNAs and not siRNAs).

d, Caffeine resistance depends on RNAi. *dcr1*$^{+}$ (*dcr1Δ*), *ago1*$^{+}$ (*ago1Δ*) or an unlinked intergenic region (*control1Δ*) were deleted in UR-2 cells. Experiment was independently repeated at least twice with similar results.

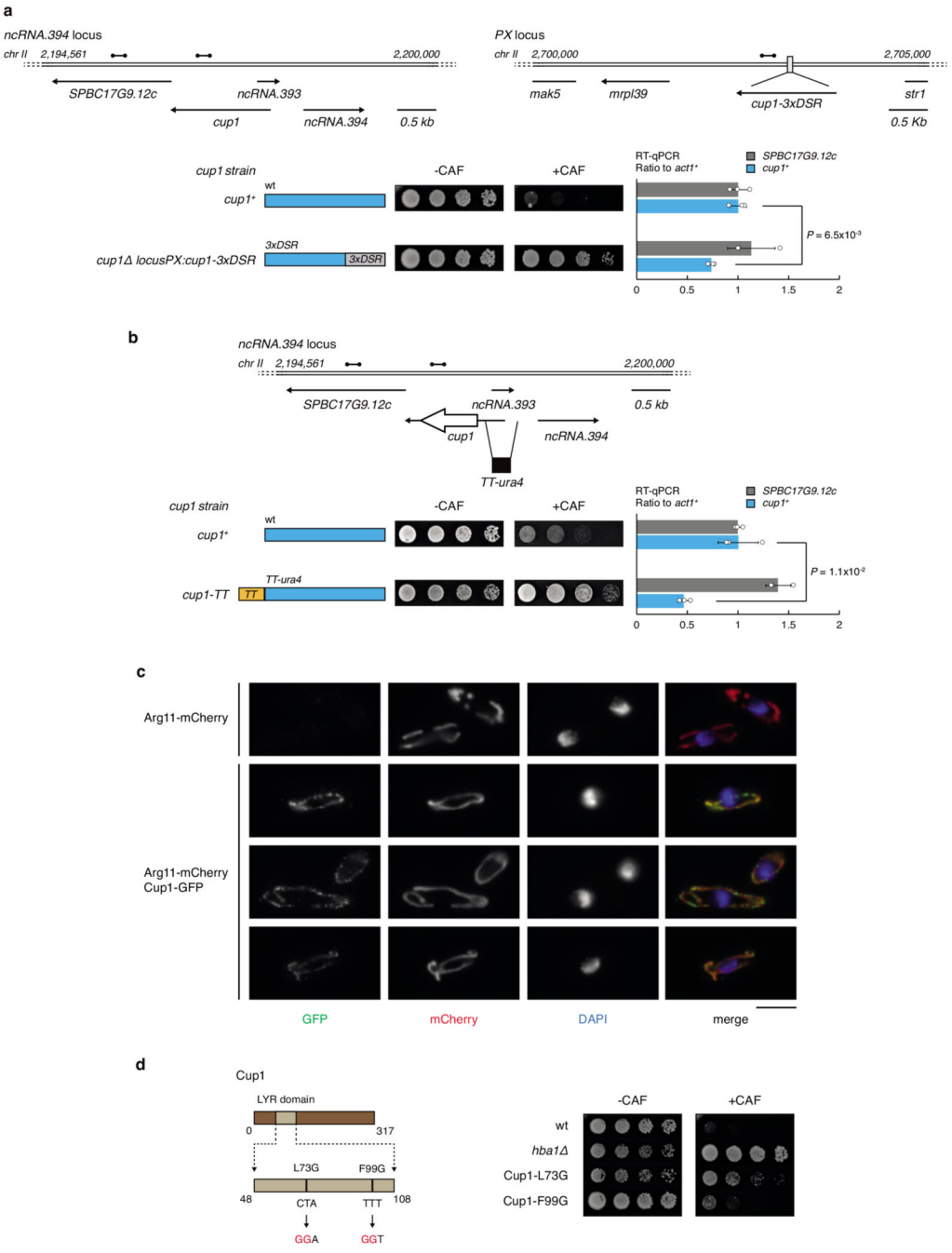

Europe PMC Funders Author Manuscripts

Europe PMC Funders Author Manuscripts

Extended Data Figure 6. Decreased *cup1*$^+$ transcript levels or Cup1 LYR-domain mutation results in caffeine resistance

a, An additional copy of *cup1*$^+$ with 3x Determinant of Selective Removal (DSR) motifs fused to its 3' untranslated region was inserted at an intergenic region (*LocusPX:cup1-3xDSR*). *Bottom left*: After deletion of endogenous *cup1*$^+$, cells expressing only *cup1-3xDSR* were assessed for caffeine resistance. *Bottom right*: Transcript levels of *cup1*$^+$ and *SPBC17G9.12c*$^+$ (as control) in *cup1Δ locusPX:cup1-3xDSR* cells compared to wild-type. Data are mean ± s.d. from three biological replicates. *P* value from a two-tailed Student's *t*-test is indicated. Dumbbells indicate primer pairs used.

b, The 144-bp transcriptional terminator site from *ura4*$^+$ was inserted in place of part of the putative *cup1*$^+$ promoter (*cup1-TT*). *Bottom left*: Cells were assessed for caffeine resistance. *Bottom right*: Transcript levels of *cup1*$^+$ and *SPBC17G9.12c*$^+$ (as control) in *cup1-TT* cells compared to wild type. Data are mean ± s.d. from three biological replicates. *P* value from a two-tailed Student's *t*-test is indicated. Dumbbells indicate primer pairs used.

c, Cup1 localises to mitochondria. Cells expressing either untagged Cup1 (top row) or Cup1-GFP (bottom three rows) were fixed and processed for immunofluorescence with anti-GFP antibody and Alexa-488 secondary antibody and DNA was stained with DAPI. The mitochondrial protein Arg11-mCherry served as a positive control for mitochondrial localisation. All images in the green channel (Cup1-GFP) are scaled relative to each other, as are those in the red channel (Arg11-mCherry); DAPI images are autoscaled. Bar, 5 μm.

d, Point mutations (L73G and F99G) were introduced in the LYR domain of Cup1 and cells were assessed for caffeine resistance. Mutations were designed based on *Phyre2* tool analysis. *hba1Δ* cells were used as positive control.

Experiments in (**c**) and (**d**) were independently repeated at least twice with similar results.

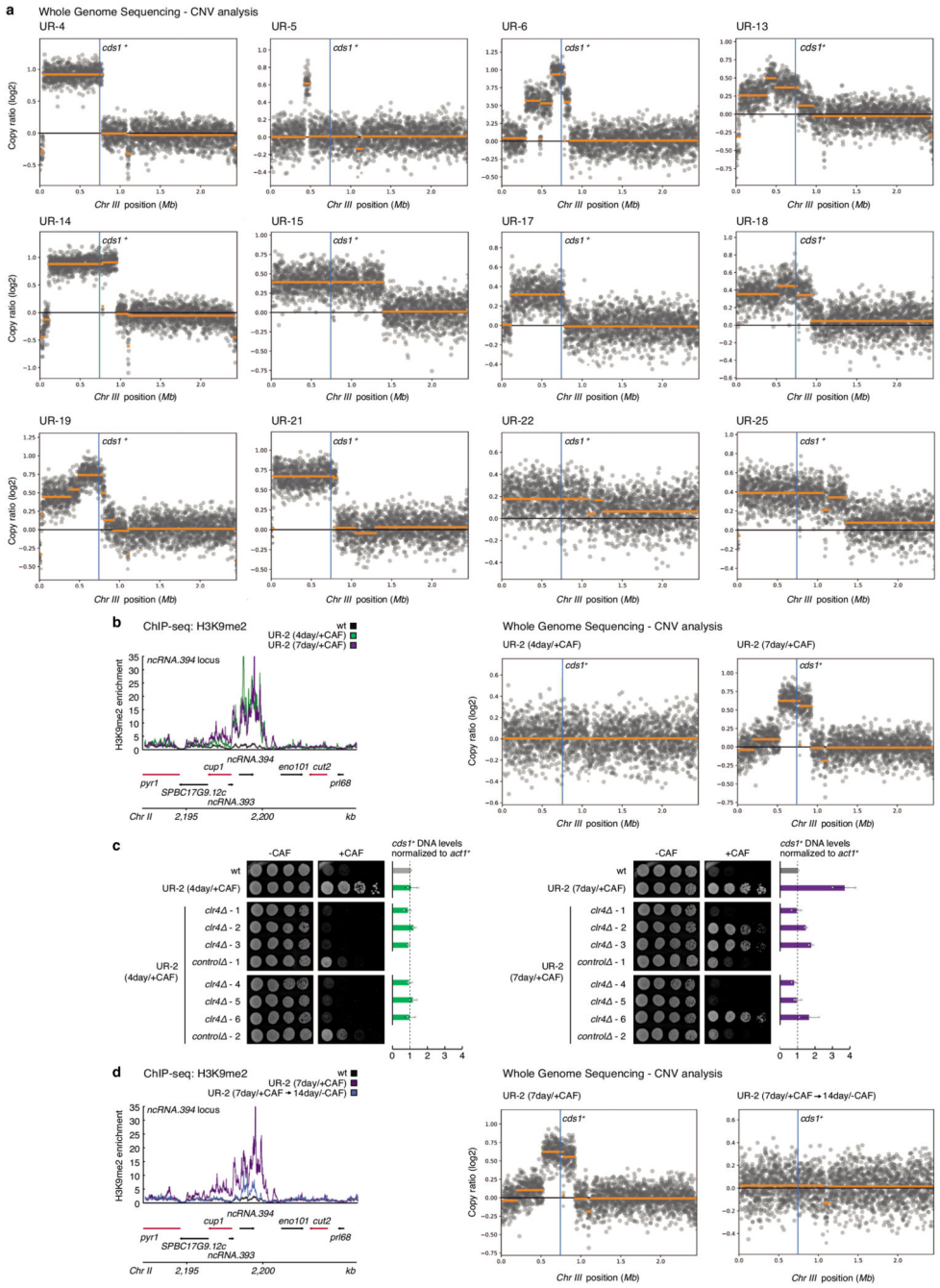

Extended Data Figure 7. Copy Number Variation (CNV) analysis reveals a partial duplication of chromosome III in 12 of 30 unstable (UR) caffeine-resistant isolates

a, Chromosome III coverage plots with overlaid segments in UR isolates showing partial duplication of chromosome III. Location of *cds1*$^{+}$ is highlighted. Wild-type ChIP-seq input data were used as the reference.

b-d, Epigenetic changes preceded genetic changes (CNV) in unstable caffeine-resistant isolate UR-2.

b, H3K9me2 ChIP-seq enrichment at the *ncRNA.394/cup1* locus (*left*) and chromosome III coverage plots with overlaid segments (*right*) in UR-2 (4day/+CAF) cells and following their prolonged growth on +CAF for an additional 3 days (7day/+CAF). Wild-type ChIP-seq input data were used as the reference for CNV analysis.

c, *clr4*$^{+}$ (*clr4Δ*) or an unlinked intergenic region (*controlΔ*) were deleted in UR-2 cells (4day/+CAF) and UR-2 (7day/+CAF). All (6/6) UR-2 (4day/+CAF) *clr4Δ* transformants lost resistance to caffeine whereas only 50% (3/6, transformants 1, 4 and 5) UR-2 (7day/+CAF) lost resistance to caffeine. Experiments were independently repeated at least twice with similar results. *cds1*$^{+}$ DNA levels in extracted genomic DNA were assessed by qPCR. Data are mean ± s.d. from three biological replicates.

d, H3K9me2 ChIP-seq enrichment at the *ncRNA.394/cup1* locus (*left*) and chromosome III coverage plots with overlaid segments (*right*) in UR-2 (7day/+CAF) cells and following their prolonged growth on non-selective media for 14 days (7day/+CAFà14day/-CAF). Wild-type ChIP-seq input data were used as the reference for CNV analysis.

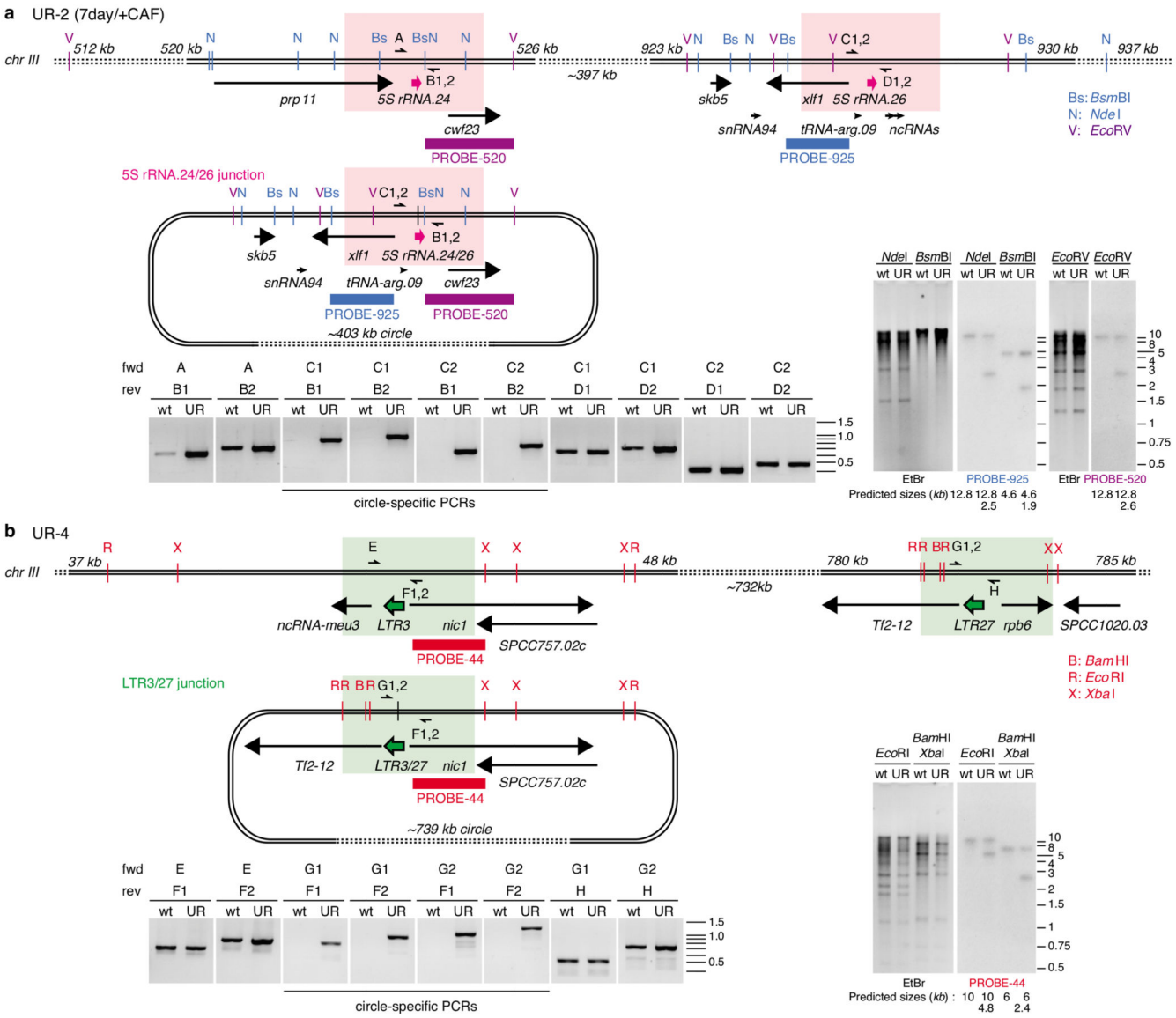

Extended Data Figure 8. Copy Number Variation (CNV) of chromosome III corresponds to extrachromosomal circular DNA (eccDNA)

Junctions of putative extrachromosomal circles were identified at repetitive sequences by inspection of CNV plots for UR-2 (7day/+CAF) (**a**) and UR-4 (**b**). *Maps and lower panels*: Positions of *5S rRNA.24* and *5S rRNA.26* (pink arrows), *LTR3* and *LTR27* (green arrows) and flanking genes are indicated. PCR primers (half arrows) flanking *5S rRNA.24* (A (forward); B1,2 (reverse)) and *5S rRNA.26* (C1,2; D1,2) were used to amplify products from wild-type (wt) and UR-2 (7day/+CAF) ChIP input samples, along with primer combinations (C1,2; B1,2) specific for the putative circle junctions (vertical black lines). Primers flanking *LTR3* (E; F1,2) and *LTR27* (G1,2; H) were used to amplify products from wild-type and UR-4 ChIP input samples, along with primer combinations (G1,2; F1,2) specific for the putative circle junction. Shaded boxes indicate primer locations and predicted circle junctions (pink: *5S rRNA.24/26*, green: *LTR3/27*). *Right*: Restriction enzyme-digested

Europe PMC Funders Author Manuscripts

genomic DNA isolated from wild-type (wt), UR-2 (7day/+CAF) and UR-4 was separated on an Ethidium Bromide (EtBr)-containing gel followed by Southern analysis using the indicated probes (925: blue; 520: purple; 44: red). Relevant restriction enzyme sites are indicated. Predicted sizes of hybridising fragments and DNA size markers are indicated (kb). PCR experiments were independently repeated at least twice with similar results. For gel source data, see Supplementary Figure 1b.

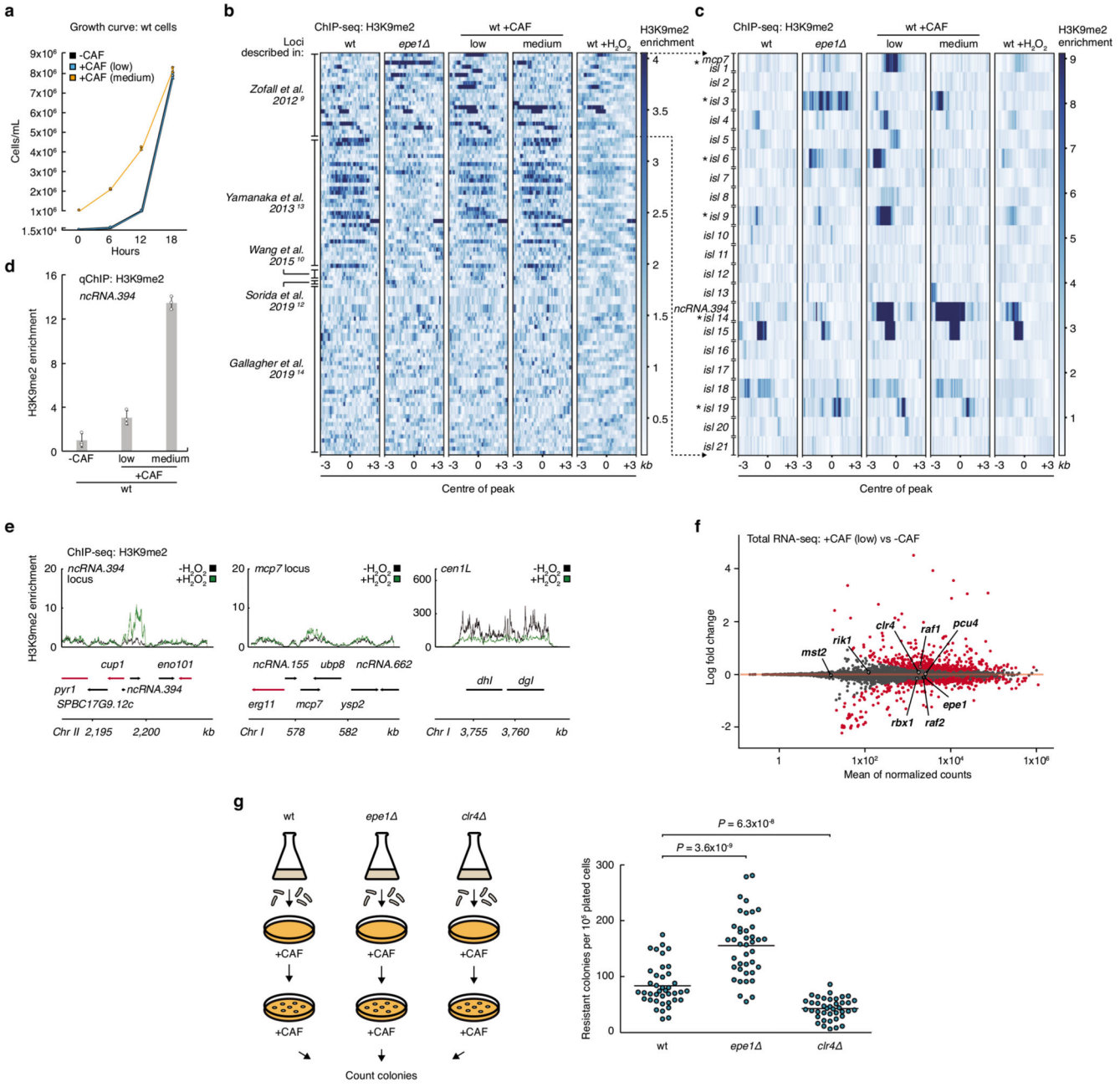

Extended Data Figure 9. The heterochromatin profile of low caffeine-treated wild-type cells resembles that of untreated *epe1*Δ cells

Europe PMC Funders Author Manuscripts

a, Growth of cells in caffeine. Wild-type (wt) cells were grown in the presence of low (7 mM) or medium (14 mM) caffeine for 18 hours. Cell number was counted every 6 hours. Note: a larger inoculum was used for 14 mM caffeine culture to obtain an equivalent final number of cells. Data are mean ± s.d. from three biological replicates. Cells from the 18-hr time point were used for **d**.

b-c, H3K9me2 ChIP-seq enrichment at previously-detected facultative heterochromatin loci (described in Zofall *et al.*, 2012[9] (**b** and **c**), Yamanaka *et al.*, 2013[13] (**b**), Wang *et al.*, 2015[10] (**b**), Sorida *et al.*, 2019[12] (**b**) and Gallagher *et al.*, 2019[14] (**b**)), in wt cells treated with low or medium dose of caffeine or low dose (1 mM) of H_2O_2, compared to untreated *epe1Δ* and wt cells. Data are represented as relative fold enrichment over input. A subset of facultative heterochromatin loci detected in untreated *epe1Δ* cells (Zofall *et al.*, 2012[9], Wang *et al.*, 2015[10] and Sorida *et al.*, 2019[12]) was detected in low caffeine-treated wt cells. Asterisks in **c** indicate loci with similar H3K9me2 patterns in low caffeine-treated wt cells and untreated *epe1Δ* cells, but not untreated wt cells. Facultative heterochromatin loci formed in the absence of the exosome (Yamanaka *et al.*, 2013[13]) or in wt cells grown at 18°C (Gallagher *et al.*, 2019[14]) were not detected in wt cells treated with low or medium caffeine or low H_2O_2.

d, Quantitative ChIP (qChIP) of H3K9me2 levels on *ncRNA.394/cup1* in wt cells following 18 hr exposure to low or medium caffeine. H3K9me2 levels were normalized to *S. octosporus* spike-in control. Data are mean ± s.d. from three biological replicates.

e, H3K9me2 ChIP-seq enrichment at *ncRNA.394/cup1* and *mcp7* loci (or at pericentromeric *dgI/dhI* repeats of chromosome I as control) in wt cells following 18 hr exposure to low H_2O_2. Data are represented as relative fold enrichment over input. Red arrows indicate essential genes. Lower levels of H3K9me2 at pericentromeric repeats upon H_2O_2 treatment may be due to H_2O_2-specific regulation of limiting heterochromatin factors at this locus.

f, *epe1*$^+$ RNA levels do not change upon caffeine treatment. Total RNA-seq of wt cells treated with low caffeine. Components of the Clr4 H3K9 methyltransferase CLRC complex (*clr4*$^+$*, rik1*$^+$*, raf1*$^+$*, raf2*$^+$*, pcu4*$^+$ *and rbx1*$^+$*)* and the antisilencing factors *epe1*$^+$ *and mst2*$^+$ are highlighted. Experiment was independently repeated twice with similar results.

g, *epe1Δ* cells display increased resistance to caffeine. *Left*: Schematic of experiment. Wild-type, *epe1Δ* and *clr4Δ* cells were plated on +CAF media (10^5 cells/plate, 40 plates/strain). Caffeine-resistant colonies were counted after 7 days. *Right*: Compared to wt cells, *epe1Δ* forms more, whereas *clr4Δ* forms fewer, caffeine-resistant colonies. Note that the total number of resistant colonies also includes genetic mutants. Data are mean from forty technical replicates. *P* values from a two-tailed Student's *t*-test are indicated.

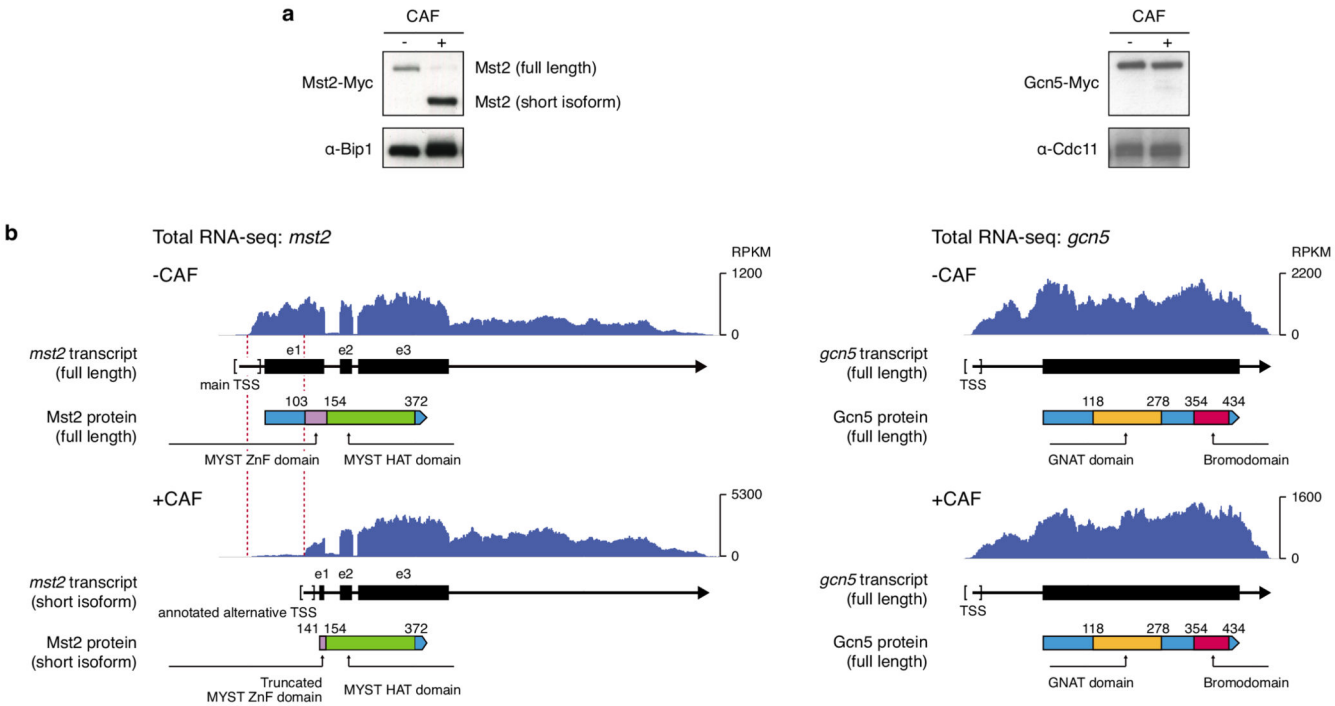

Extended Data Figure 10. A shortened version of the anti-silencing factor Mst2 is produced upon exposure to caffeine

a, Western analysis of Mst2-13xMyc (*left*) and Gcn5-13xMyc (as HAT control, *right*) before and after caffeine treatment (medium concentration, 14 mM). Tagged proteins are expressed from their endogenous loci. Loading controls: *left*: Bip1; *right*: Cdc11. Experiments were independently repeated at least twice with similar results. For gel source data, see Supplementary Figure 1c.

b, Total RNA-seq for *mst2 (left)* and *gcn5* (as HAT control, *right*) of untreated wild-type cells (*top*) or wild-type cells treated with medium caffeine concentration (*bottom*). Diagrams illustrate *mst2* and *gcn5* transcripts and predicted protein domains. Reads are normalized to RPKM. Red dashed lines indicate the region of full length *mst2* transcript absent from the short isoform. The MYST zinc finger (ZnF) domain, required for *S. cerevisiae* Esa1 acetyltransferase activity[29], is truncated in the short isoform of Mst2. The alternative *mst2* TSS utilised in caffeine conditions was previously annotated[28]. Experiment was independently repeated twice with similar results.

Supplementary Material

Refer to Web version on PubMed Central for supplementary material.

Acknowledgments

We thank Lorenza Di Pompeo, Andreas Fellas and Rebecca Yeboah for laboratory support, Pin Tong, Marcel Lafos, Ryan Ard and Shaun Webb (Wellcome Centre for Cell Biology Bioinformatics Core) for sharing technical expertise, David Kelly (Wellcome Centre Optical Instrumentation Laboratory) for microscopy and instrumentation support, and members of the Allshire lab for valuable discussions. We are grateful to Adrian Bird, Wendy Bickmore and Lucia Massari for comments on the manuscript. We thank Takeshi Urano for the 5.1.1 (H3K9me) antibody, Yoshinori Watanabe for the pRAD21 plasmid, Keith Gull for the α-tubulin antibody, Adele Marston for the Sgo1-

GFP *S. cerevisiae* strain, Ken Sawin for the Cdc11 antibody and both Edinburgh Genomics (NERC, R8/H10/56; MRC, MR/K001744/1; BBSRC, BB/J004243/1) and Genetics Core, Edinburgh Clinical Research Facility at the University of Edinburgh for sequencing. S.T-G. was supported by the Darwin Trust of Edinburgh. R.C.A. is a Wellcome Principal Research Fellow (095021, 200885); the Wellcome Centre for Cell Biology is supported by core funding from Wellcome (203149).

Data availability

Sequence data generated in this study have been submitted to GEO under accession number: GSE138436.

Code availability

The complete Workflow Description Language (WDL) pipeline script used for ChIP-seq and variation analyses is available at: https://github.com/SitoTorres/Torres-Garcia-et-al.-2019.

References

1. Bannister AJ, et al. Selective recognition of methylated lysine 9 on histone H3 by the HP1 chromo domain. Nature. 2001; 410:120–124. [PubMed: 11242054]
2. Lachner M, O'Carroll D, Rea S, Mechtler K, Jenuwein T. Methylation of histone H3 lysine 9 creates a binding site for HP1 proteins. Nature. 2001; 410:116–120. [PubMed: 11242053]
3. Allshire RC, Madhani HD. Ten principles of heterochromatin formation and function. Nat Rev Mol Cell Biol. 2017; 45:153.
4. Audergon PNCB, et al. Epigenetics. Restricted epigenetic inheritance of H3K9 methylation. Science. 2015; 348:132–135. [PubMed: 25838386]
5. Ragunathan K, Jih G, Moazed D. Epigenetics. Epigenetic inheritance uncoupled from sequence-specific recruitment. Science. 2015; 348
6. Jeggo PA, Holliday R. Azacytidine-induced reactivation of a DNA repair gene in Chinese hamster ovary cells. Mol Cell Biol. 1986; 6:2944–2949. [PubMed: 2431295]
7. Oey H, Whitelaw E. On the meaning of the word 'epimutation'. Trends Genet. 2014; 30:519–520. [PubMed: 25301328]
8. Zhang K, Mosch K, Fischle W, Grewal SIS. Roles of the Clr4 methyltransferase complex in nucleation, spreading and maintenance of heterochromatin. Nat Struct Mol Biol. 2008; 15:381–388. [PubMed: 18345014]
9. Zofall M, et al. RNA elimination machinery targeting meiotic mRNAs promotes facultative heterochromatin formation. Science. 2012; 335:96–100. [PubMed: 22144463]
10. Wang J, Reddy BD, Jia S. Rapid epigenetic adaptation to uncontrolled heterochromatin spreading. eLife. 2015; 4:80.
11. Parsa J-Y, Boudoukha S, Burke J, Homer C, Madhani HD. Polymerase pausing induced by sequence-specific RNA-binding protein drives heterochromatin assembly. Genes Dev. 2018; 32:953–964. [PubMed: 29967291]
12. Sorida M, et al. Regulation of ectopic heterochromatin-mediated epigenetic diversification by the JmjC family protein Epe1. PLoS Genet. 2019; 15:e1008129. [PubMed: 31206516]
13. Yamanaka S, et al. RNAi triggered by specialized machinery silences developmental genes and retrotransposons. Nature. 2013; 493:557–560. [PubMed: 23151475]
14. Gallagher PS, et al. Iron homeostasis regulates facultative heterochromatin assembly in adaptive genome control. Nat Struct Mol Biol. 2018; 25:372–383. [PubMed: 29686279]
15. Calvo IA, et al. Genome-wide screen of genes required for caffeine tolerance in fission yeast. PLoS ONE. 2009; 4:e6619. [PubMed: 19672306]
16. Ivanova AV, Bonaduce MJ, Ivanov SV, Klar AJ. The chromo and SET domains of the Clr4 protein are essential for silencing in fission yeast. Nat Genet. 1998; 19:192–195. [PubMed: 9620780]

Europe PMC Funders Author Manuscripts

17. Nakayama J, Rice JC, Strahl BD, Allis CD, Grewal SI. Role of histone H3 lysine 9 methylation in epigenetic control of heterochromatin assembly. Science. 2001; 292:110–113. [PubMed: 11283354]
18. Kudo N, Taoka H, Toda T, Yoshida M, Horinouchi S. A novel nuclear export signal sensitive to oxidative stress in the fission yeast transcription factor Pap1. J Biol Chem. 1999; 274:15151–15158. [PubMed: 10329722]
19. Castillo EA, Vivancos AP, Jones N, Ayté J, Hidalgo E. *Schizosaccharomyces pombe* cells lacking the Ran-binding protein Hba1 show a multidrug resistance phenotype due to constitutive nuclear accumulation of Pap1. J Biol Chem. 2003; 278:40565–40572. [PubMed: 12896976]
20. Zofall M, Smith DR, Mizuguchi T, Dhakshnamoorthy J, Grewal SIS. Taz1-Shelterin Promotes Facultative Heterochromatin Assembly at Chromosome-Internal Sites Containing Late Replication Origins. Mol Cell. 2016; 62:862–874. [PubMed: 27264871]
21. Angerer H. Eukaryotic LYR Proteins Interact with Mitochondrial Protein Complexes. Biology. 2015; 4:133–150. [PubMed: 25686363]
22. Wang SW, Norbury C, Harris AL, Toda T. Caffeine can override the SM checkpoint in fission yeast. J Cell Sci. 1999; 112:927–937. [PubMed: 10036242]
23. Libuda DE, Winston F. Amplification of histone genes by circular chromosome formation in Saccharomyces cerevisiae. Nature. 2006; 443:1003–1007. [PubMed: 17066037]
24. Møller HD, Parsons L, Jørgensen TS, Botstein D, Regenberg B. Extrachromosomal circular DNA is common in yeast. Proc Natl Acad Sci USA. 2015; 112:E3114–22. [PubMed: 26038577]
25. Hull RM, et al. Transcription-induced formation of extrachromosomal DNA during yeast ageing. PLoS Biol. 2019; 17:e3000471. [PubMed: 31794573]
26. Wu S, et al. Circular ecDNA promotes accessible chromatin and high oncogene expression. Nature. 2019; 575:699–703. [PubMed: 31748743]
27. Stajic D, Perfeito L, Jansen LET. Epigenetic gene silencing alters the mechanisms and rate of evolutionary adaptation. Nat Ecol Evol. 2019; 3:491–498. [PubMed: 30718851]
28. Thodberg M, et al. Comprehensive profiling of the fission yeast transcription start site activity during stress and media response. Nucleic Acids Res. 2019; 47:1671–1691. [PubMed: 30566651]
29. Yan Y, Barlev NA, Haley RH, Berger SL, Marmorstein R. Crystal structure of yeast Esa1 suggests a unified mechanism for catalysis and substrate binding by histone acetyltransferases. Mol Cell. 2000; 6:1195–1205. [PubMed: 11106757]
30. Cubas P, Vincent C, Coen E. An epigenetic mutation responsible for natural variation in floral symmetry. Nature. 1999; 401:157–161. [PubMed: 10490023]
31. Heard E, Martienssen RA. Transgenerational epigenetic inheritance: myths and mechanisms. Cell. 2014; 157:95–109. [PubMed: 24679529]
32. Calo S, et al. Antifungal drug resistance evoked via RNAi-dependent epimutations. Nature. 2014; 513:555–558. [PubMed: 25079329]
33. Antequera F, Tamame M, Villanueva JR, Santos T. DNA methylation in the fungi. J Biol Chem. 1984; 259:8033–8036. [PubMed: 6330093]
34. Wilkinson CR, Bartlett R, Nurse P, Bird AP. The fission yeast gene pmt1^{+} encodes a DNA methyltransferase homologue. Nucleic Acids Res. 1995; 23:203–210. [PubMed: 7862522]
35. Fisher MC, Hawkins NJ, Sanglard D, Gurr SJ. Worldwide emergence of resistance to antifungal drugs challenges human health and food security. Science. 2018; 360:739–742. [PubMed: 29773744]
36. Moreno S, Klar A, Nurse P. Molecular genetic analysis of fission yeast *Schizosaccharomyces pombe* . Meth Enzymol. 1991; 194:795–823.
37. Harigaya Y, et al. Selective elimination of messenger RNA prevents an incidence of untimely meiosis. Nature. 2006; 442:45–50. [PubMed: 16823445]
38. Watson AT, et al. Optimisation of the *Schizosaccharomyces pombe* urg1 expression system. PLoS ONE. 2013; 8:e83800. [PubMed: 24376751]
39. Delerue T, et al. Loss of Msp1p in *Schizosaccharomyces pombe* induces a ROS-dependent nuclear mutator phenotype that affects mitochondrial fission genes. FEBS Lett. 2016; 590:3544–3558. [PubMed: 27664110]

40. Bähler J, et al. Heterologous modules for efficient and versatile PCR-based gene targeting in *Schizosaccharomyces pombe* . Yeast. 1998; 14:943–951. [PubMed: 9717240]
41. Tong P, et al. Interspecies conservation of organisation and function between nonhomologous regional centromeres. Nat Commun. 2019; 10
42. Nerusheva OO, Galander S, Fernius J, Kelly D, Marston AL. Tension-dependent removal of pericentromeric shugoshin is an indicator of sister chromosome biorientation. Genes Dev. 2014; 28:1291–1309. [PubMed: 24939933]
43. Bolger AM, Lohse M, Usadel B. Trimmomatic: a flexible trimmer for Illumina sequence data. Bioinformatics. 2014; 30:2114–2120. [PubMed: 24695404]
44. Langmead B, Salzberg SL. Fast gapped-read alignment with Bowtie 2. Nat Methods. 2012; 9:357–359. [PubMed: 22388286]
45. Li H, et al. The Sequence Alignment/Map format and SAMtools. Bioinformatics. 2009; 25:2078–2079. [PubMed: 19505943]
46. Ramírez F, et al. deepTools2: a next generation web server for deep-sequencing data analysis. Nucleic Acids Res. 2016; 44:W160–5. [PubMed: 27079975]
47. Diaz A, Park K, Lim DA, Song JS. Normalization, bias correction, and peak calling for ChIP-seq. Stat Appl Genet Mol Biol. 2012; 11
48. Zhang Y, et al. Model-based analysis of ChIP-Seq (MACS). Genome Biol. 2008; 9:R137. [PubMed: 18798982]
49. Phanstiel DH, Boyle AP, Araya CL, Snyder MP. Sushi.R: flexible, quantitative and integrative genomic visualizations for publication-quality multi-panel figures. Bioinformatics. 2014; 30:2808–2810. [PubMed: 24903420]
50. Jeffares DC, et al. The genomic and phenotypic diversity of *Schizosaccharomyces pombe* . Nat Genet. 2015; 47:235–241. [PubMed: 25665008]
51. McKenna A, et al. The Genome Analysis Toolkit: a MapReduce framework for analyzing next-generation DNA sequencing data. Genome Res. 2010; 20:1297–1303. [PubMed: 20644199]
52. Van der Auwera GA, et al. From FastQ data to high confidence variant calls: the Genome Analysis Toolkit best practices pipeline. Curr Protoc Bioinformatics. 2013; 43
53. McLaren W, et al. The Ensembl Variant Effect Predictor. Genome Biol. 2016; 17:122. [PubMed: 27268795]
54. Talevich E, Shain AH, Botton T, Bastian BC. CNVkit: Genome-Wide Copy Number Detection and Visualization from Targeted DNA Sequencing. PLoS Comput Biol. 2016; 12:e1004873. [PubMed: 27100738]
55. Dobin A, et al. STAR: ultrafast universal RNA-seq aligner. Bioinformatics. 2013; 29:15–21. [PubMed: 23104886]
56. Lawrence M, et al. Software for computing and annotating genomic ranges. PLoS Comput Biol. 2013; 9:e1003118. [PubMed: 23950696]
57. Love MI, Huber W, Anders S. Moderated estimation of fold change and dispersion for RNA-seq data with DESeq2. Genome Biol. 2014; 15:550. [PubMed: 25516281]
58. Zhu A, Ibrahim JG, Love MI. Heavy-tailed prior distributions for sequence count data: removing the noise and preserving large differences. Bioinformatics. 2019; 35:2084–2092. [PubMed: 30395178]
59. Fletcher SJ, Boden M, Mitter N, Carroll BJ. SCRAM: a pipeline for fast index-free small RNA read alignment and visualization. Bioinformatics. 2018; 34:2670–2672. [PubMed: 29554210]
60. Braun S, et al. The Cul4-Ddb1(Cdt)^2 ubiquitin ligase inhibits invasion of a boundary-associated antisilencing factor into heterochromatin. Cell. 2011; 144:41–54. [PubMed: 21215368]
61. Woods A, et al. Definition of individual components within the cytoskeleton of Trypanosoma brucei by a library of monoclonal antibodies. J Cell Sci. 93(Pt 3):491–500.1989; [PubMed: 2606940]
62. Pidoux AL, Armstrong J. The BiP protein and the endoplasmic reticulum of *Schizosaccharomyces pombe*: fate of the nuclear envelope during cell division. J Cell Sci. 105(Pt 4):1115–1120.1993; [PubMed: 8227200]

Europe PMC Funders Author Manuscripts

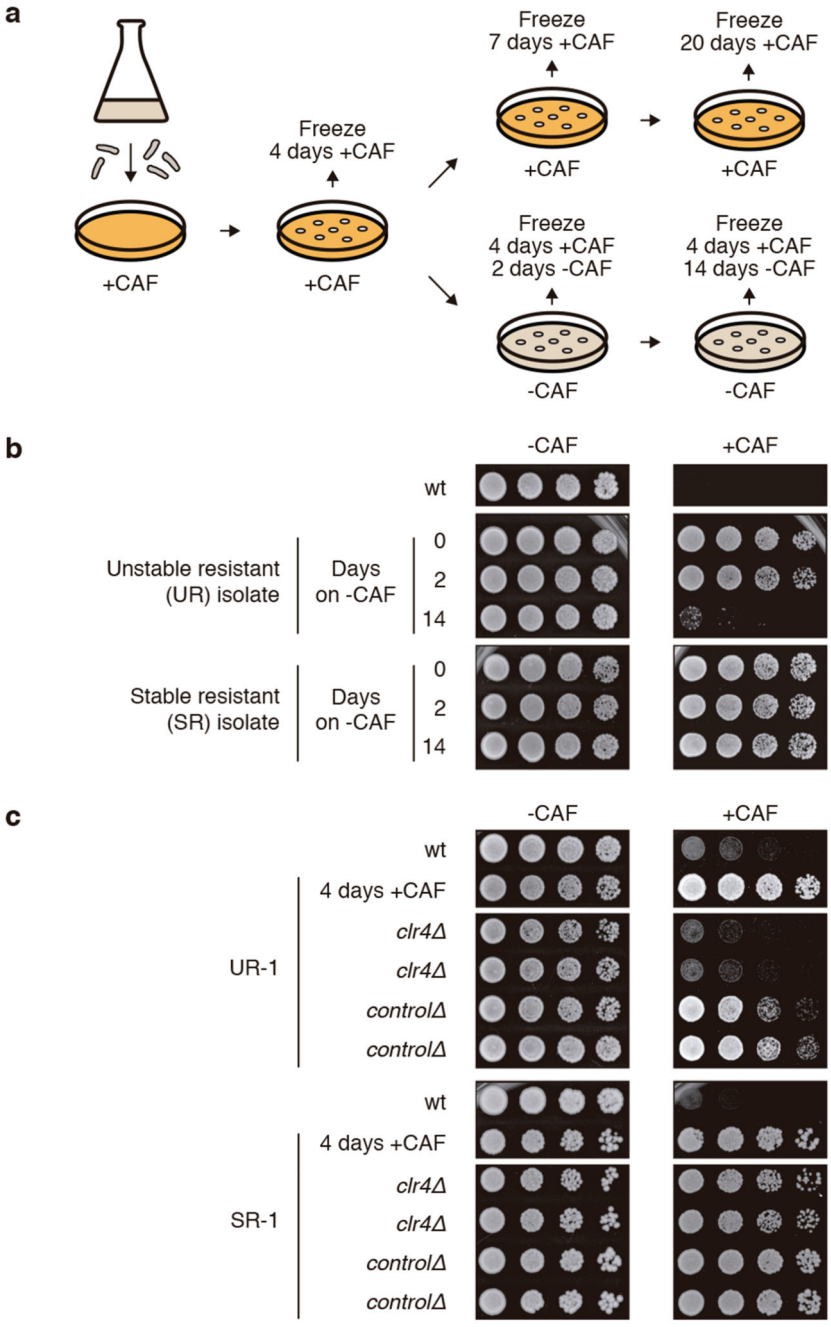

Figure 1. Identification of heterochromatin-dependent epimutants resistant to caffeine

a, Screening strategy. *S. pombe* wild-type (wt) cells were plated on caffeine-containing (+CAF) media. Caffeine-resistant isolates were picked and grown on +CAF for 4 days. Isolates were then grown on +CAF for a total of 7 or 20 days or on non-selective (-CAF) media for 2 and 14 days.

b, Unstable (UR) and stable (SR) caffeine-resistant isolates were identified. After non-selective growth for 2 and 14 days, caffeine-resistant isolates were serially diluted and spotted on -CAF and +CAF plates to assess resistance to caffeine.

c, Caffeine resistance in UR isolates depends on the Clr4 H3K9 methyltransferase. *clr4*$^{+}$ (*clr4Δ*) or an unlinked intergenic region (*control Δ*) were deleted in unstable (UR-1) and stable (SR-1) caffeine-resistant isolates.

Experiments in (**b**) and (**c**) were independently repeated at least twice with similar results.

Europe PMC Funders Author Manuscripts

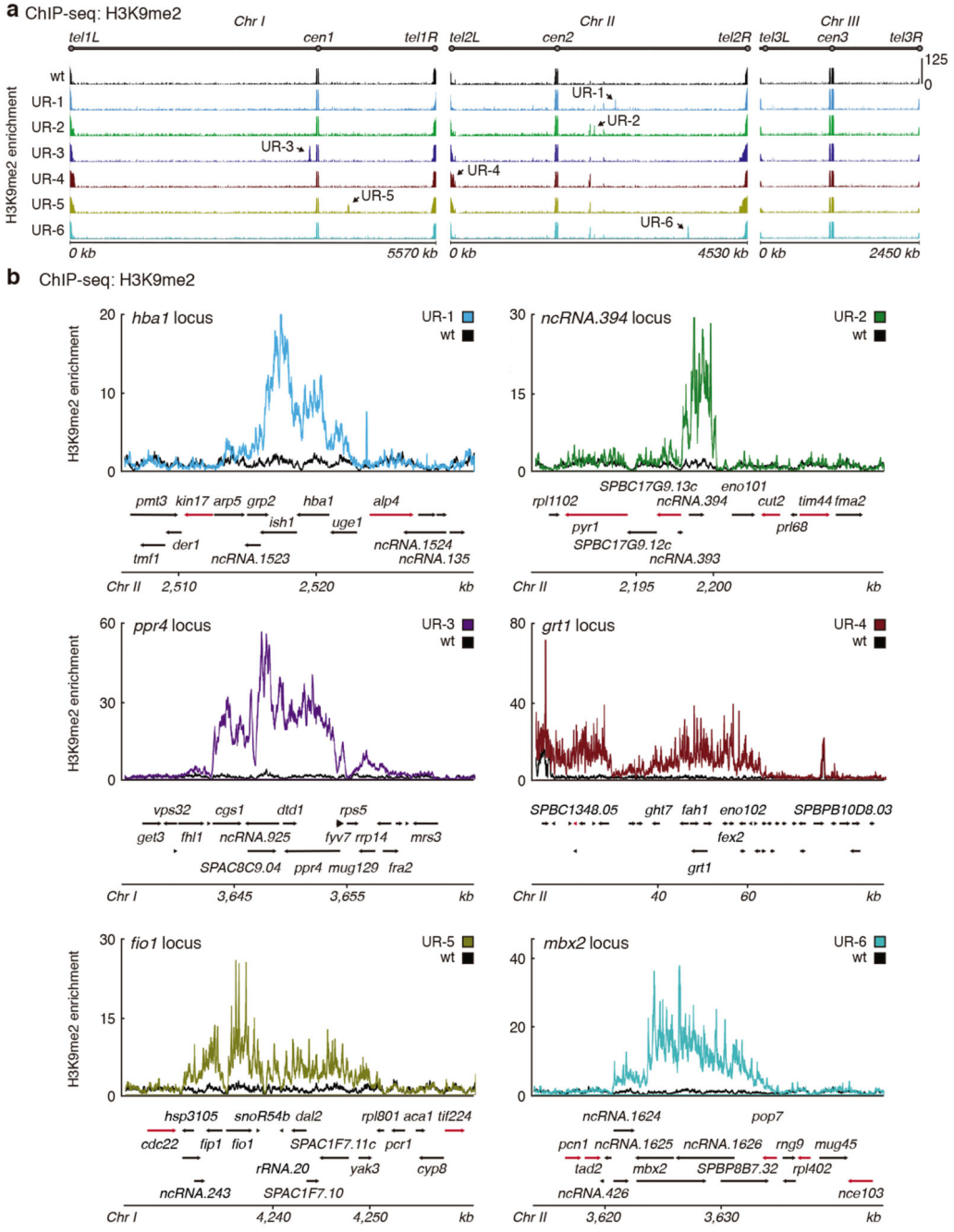

Figure 2. Ectopic islands of heterochromatin are detected in unstable (UR) caffeine-resistant isolates

a-b, Genome-wide (**a**) and locus-specific (**b**) H3K9me2 ChIP-seq enrichment in wild-type (wt) cells and UR isolates. Data are represented as relative fold enrichment over input. Sequencing was performed once, and results were confirmed by qChIP. Red arrows in (**b**) indicate essential genes.

Europe PMC Funders Author Manuscripts

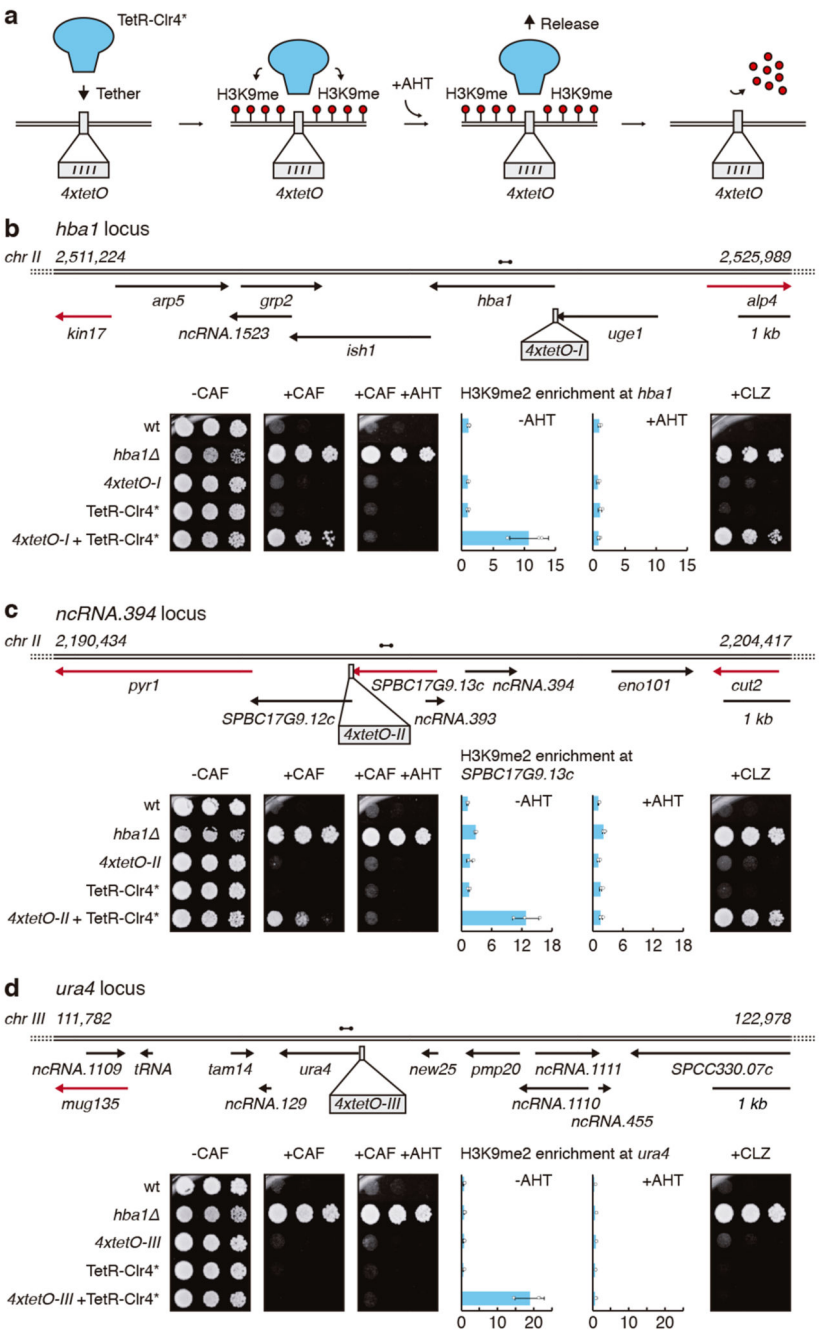

Figure 3. Forced synthetic heterochromatin targeting to the identified loci is sufficient to drive caffeine resistance in wild-type cells

a, TetR-Clr4* mediates H3K9me deposition at *4xtetO* binding sites. Addition of anhydrotetracycline (+AHT) releases TetR-Clr4* from *4xtetO* sites, resulting in removal of H3K9me.

b-d, Wild-type (wt) cells harbouring *4xtetO* binding sites at the *hba1* or *ncRNA.394* loci (or *ura4* as control) and expressing TetR-Clr4* were assessed for caffeine (+CAF) or clotrimazole (+CLZ) resistance in the absence or presence of AHT. qChIP of H3K9me2

levels on *hba1* (**b**), *SPBC17G9.13c* (**c**) and *ura4* (**d**) loci. Data are mean ± s.d. from three biological replicates. Dumbbells indicate primer pairs used. Red arrows indicate essential genes. Note *hba1* is not present in *hba1Δ*.

Europe PMC Funders Author Manuscripts

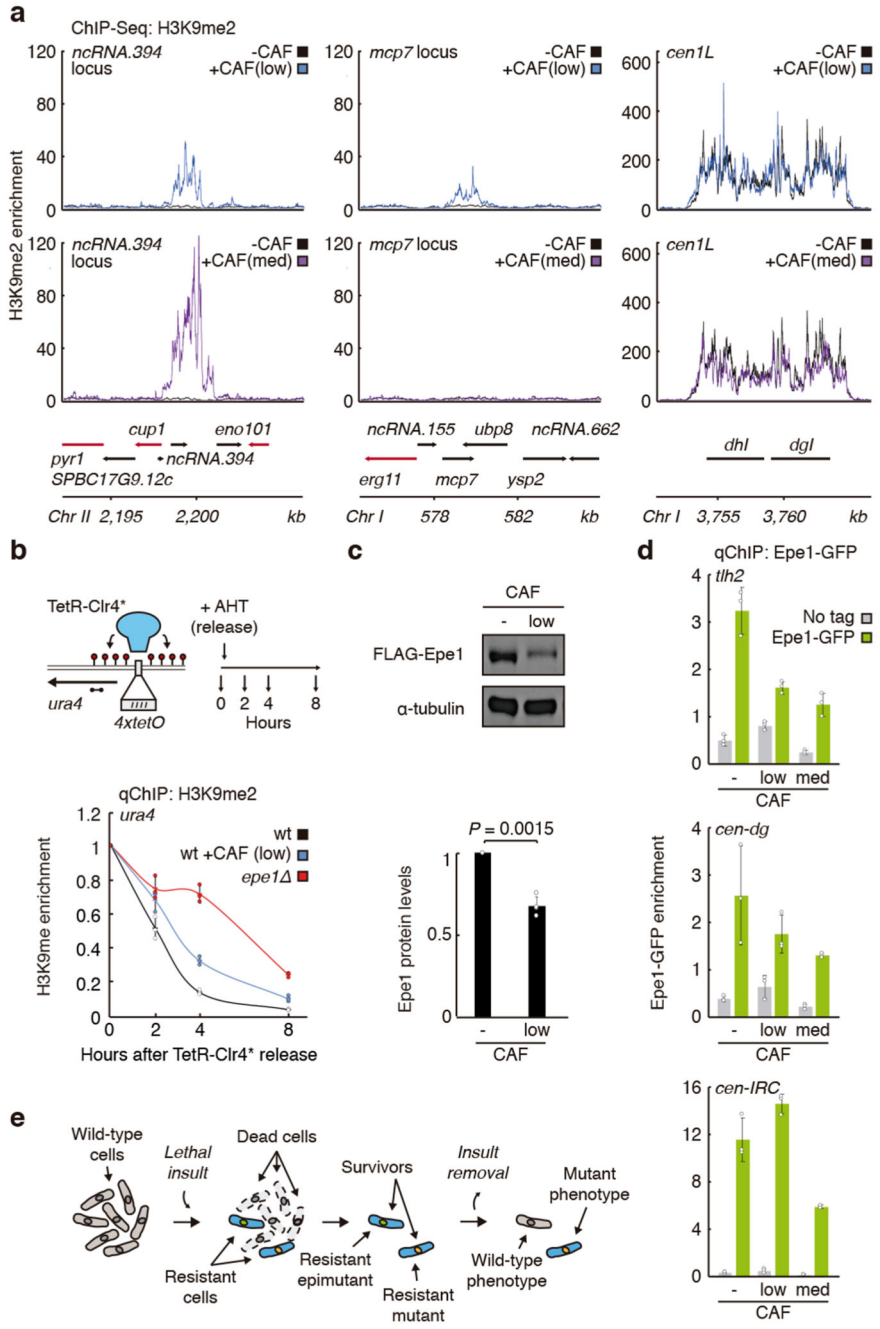

Figure 4. Dynamic heterochromatin redistribution following short exposure to caffeine in wild-type cells

a, H3K9me2 ChIP-seq enrichment at *ncRNA.394/cup1* and *mcp7* loci (or at pericentromeric *dgI/dhI* repeats of chromosome I as control) in wild-type (wt) cells following 18 hr exposure to low (7 mM, *top*) or medium (14 mM, *bottom*) concentrations of caffeine. Data are represented as relative fold enrichment over input. Red arrows indicate essential genes.

b, Effect of caffeine treatment on retention of synthetic heterochromatin upon release of tethered Clr4 methyltransferase. qChIP of H3K9me2 levels on *4xtetO-ura4*$^{+}$ before and

Europe PMC Funders Author Manuscripts

after TetR-Clr4* release in wt cells untreated or treated with low caffeine. *epe1Δ* cells were used as positive control. Dumbbells indicate primer pairs used. H3K9me2 levels were normalized to spike-in control. Data are mean ± s.d. from three biological replicates.
c, *Top*: Western analysis of 3xFLAG-Epe1 (endogenous gene tagged) levels before and after low caffeine treatment. Loading control: α-tubulin. For gel source data, see Supplementary Figure 1a.
Bottom: Quantification of 3xFLAG-Epe1 protein levels normalized to α-tubulin. Data are mean ± s.d. from four biological replicates. *P* value: two-tailed Student's *t*-test.
d, Effect of caffeine treatment on association of Epe1 with chromatin. qChIP analysis of Epe1-GFP levels at sub-telomeric *tlh2* locus and centromere 1 (*dg* repeats: *cendg*; outer boundary: *cen-IRC*) in wt cells treated with no, low or medium caffeine. Epe1-GFP levels were normalized to spike-in control. Data are mean ± s.d. from three biological replicates.
e, Model. Resistant isolates arise following exposure to a lethal insult. Resistance could be mediated by permanent, DNA-based changes (resistant mutants) or reversible, heterochromatin-based epimutations (resistant epimutants). Upon insult removal, resistant epimutants can revert to wild-type (sensitive phenotype) by disassembling ectopic heterochromatin islands, whereas resistant mutants continue displaying the mutant phenotype due to the genetic nature of DNA mutations.